HAL open science

Rainfall in the Greater and Lesser Antilles: Performance of five gridded datasets on a daily timescale

Ralph Bathelemy, Pierre Brigode, Dominique Boisson, Emmanuel Tric

To cite this version:

Ralph Bathelemy, Pierre Brigode, Dominique Boisson, Emmanuel Tric. Rainfall in the Greater and Lesser Antilles: Performance of five gridded datasets on a daily timescale. Journal of Hydrology: Regional Studies, 2022, 43, pp.101203. 10.1016/j.ejrh.2022.101203 . hal-03772033

HAL Id: hal-03772033

https://hal.science/hal-03772033v1

Submitted on 22 Sep 2022

HAL is a multi-disciplinary open access archive for the deposit and dissemination of scientific research documents, whether they are published or not. The documents may come from teaching and research institutions in France or abroad, or from public or private research centers.

L'archive ouverte pluridisciplinaire **HAL**, est destinée au dépôt et à la diffusion de documents scientifiques de niveau recherche, publiés ou non, émanant des établissements d'enseignement et de recherche français ou étrangers, des laboratoires publics ou privés.

Distributed under a Creative Commons Attribution - NonCommercial - NoDerivatives 4.0 International License

Journal of Hydrology: Regional Studies 43 (2022) 101203

Contents lists available at ScienceDirect

Journal of Hydrology: Regional Studies

journal homepage: www.elsevier.com/locate/ejrh

Rainfall in the Greater and Lesser Antilles: Performance of five gridded datasets on a daily timescale

Ralph Bathelemy [a,b,*], Pierre Brigode [a], Dominique Boisson [b], Emmanuel Tric [a]

[a] Université Côte d'Azur, Observatoire de la Côte d'Azur, CNRS, IRD, Géoazur, France
[b] Université d'Etat d'Haïti, Faculté des Sciences, LMI CARIBACT, URGéo, Haiti

ARTICLE INFO

Keywords:
Satellite rainfall
Caribbean region
Haiti
KGE
Heavy rainfall
Seasonality rainfall
Rainfall statistics
Extreme rainfall, Hispaniola, hydrology, tropical cyclone, hurricane, flood

ABSTRACT

Study region: The studied region is the Greater Antilles (Cuba, Hispaniola, Jamaica and Puerto Rico) and the Lesser Antilles (Southern part of the Caribbean arc).
Study focus: The performance of MSWEP, CHIRPS, PERSIANN-CDR, ERA-5 and GPM IMERG were evaluated to highlight their qualities and shortcomings and to guide researchers in the choice of these rainfall datasets to use for hydro-meteorological applications in this study area. Five quantitative (RMSE, KGE and his three components) and three qualitative (POD, FAR and CSI) statistical metrics are used to evaluate the amount and detection capacity of the rainfall datasets. Heavy rainfall percentiles are calculated to assess the ability of rainfall datasets to estimate rare and extreme rainfall.
New hydrological insights for the region: MSWEP performs well for most statistical metrics and is recommended for most hydro-meteorological research. CHIRPS and PERSIANN-CDR performs well in estimating the annual rainfall seasonality and are recommended for research on water resources management (irrigation, energy production, etc.). CHIRPS also performs well in estimating heavy rainfall percentiles and is also recommended for statistical research of heavy rainfall events. ERA-5 and GPM IMERG have a good ability to capture wet and dry days and is recommended for determination of climatic research or atmospheric sciences applications. However, bias reduction methods for these rainfall gridded datasets are advised before applications due to their low KGE and high RMSE.

1. Introduction

The Greater and Lesser Antilles region experienced 264 tropical cyclones between 1960 and 2013, accounting for 95 % of the total damage from all natural disasters in the region (Burgess et al., 2018). These tropical cyclones generate heavy rainfall events (Khouakhi et al., 2017) that cause large floods, whose intensities and frequency will tend to increase due to climate change (Peterson et al., 2002). Given the vulnerability of Greater and Lesser Antilles territories to hydro-meteorological hazards, rainfall databases are needed on a daily or sub-daily timescale to calculate relevant indices (e.g., the annual number of wet days above a certain threshold, 100-year rainfall maxima) to statistically characterize heavy rainfall events and to discuss their frequency and potential trends over time. Although rain gauges provide accurate local measurements of rainfall amount, they are not numerous enough in this region to reflect the high spatial and temporal variability of rainfall (Kidd et al., 2017; Villarini et al., 2008). This data scarcity is even more critical

* Corresponding author at: Université Côte d'Azur, Observatoire de la Côte d'Azur, CNRS, IRD, Géoazur, France.
E-mail address: bathelemy@geoazur.unice.fr (R. Bathelemy).

https://doi.org/10.1016/j.ejrh.2022.101203
Received 14 December 2021; Received in revised form 27 June 2022; Accepted 3 September 2022
Available online 7 September 2022
2214-5818/© 2022 The Authors. Published by Elsevier B.V. This is an open access article under the CC BY-NC-ND license (http://creativecommons.org/licenses/by-nc-nd/4.0/).

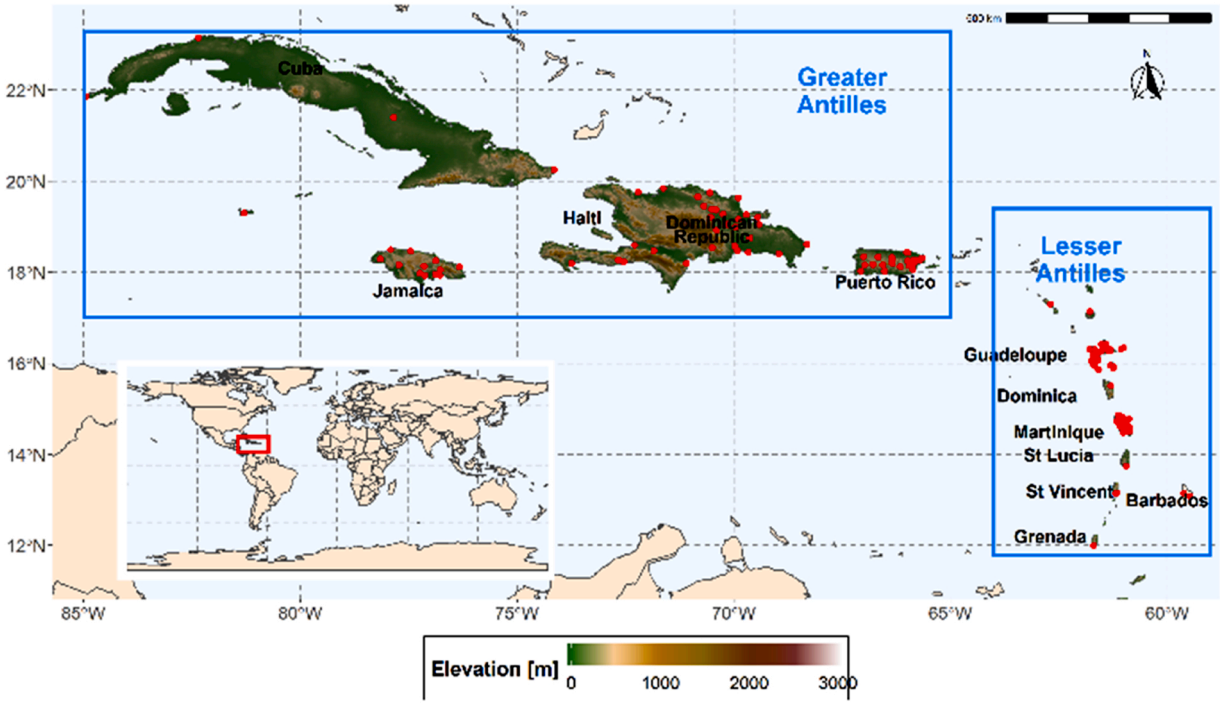

Fig. 1. Location of the rain gauges, the two studied regions (Greater and Lesser Antilles) and of the principal countries and islands studied. Elevation of the SRTM database (Jarvis et al., 2008) is plotted in the background.

when studying heavy rainfall events, which requires information on a fine spatiotemporal scale. In this context, remote sensing offers an opportunity to better study the spatiotemporal variability of precipitation (Griffith et al., 1978). Rainfall data obtained from remote sensing have the advantage of a wide spatiotemporal area coverage and have shown high potential for use in many applications (Dinku et al., 2007; Li et al., 2015), such as rainfall and flow forecasting, mapping heavy rainfall statistics, flood hazard mapping and many other hydrological applications (Mazzoleni et al., 2019; Wannasin et al., 2021).

Currently, there are more than 10 precipitation products obtained by remote sensing available in the world, covering different periods and different spatiotemporal scales (Centella-Artola et al., 2020). These remotely sensed precipitation products were created mainly from (i) satellite data (infrared observations, passive microwave observations, soil moisture observations, etc.), (ii) combinations of different data sources (satellite rainfall estimates [SRE], reanalysis rainfall products, observation data, etc.) or (iii) using atmospheric physics models coupled with reference data to create reanalysis products such as ERA-5 reanalysis. Several papers have evaluated the performance of such rainfall gridded datasets (RGD) at different spatiotemporal scales and in different climate regions (Baez-Villanueva et al., 2018; Prakash, 2019; Stampoulis and Anagnostou, 2012; Tan and Santo, 2018; Xu et al., 2017). Results indicate that the performance of the RGD is highly dependent on topography, geography and climate. Tang et al. (2019) evaluated the performance of four RGD in six climate regions in the Mekong Basin of Southeast Asia. The rainfall products were divided into seven classes, with the purpose of evaluating the ability of RGD products to estimate light and heavy rainfall in different climatic zones. The results showed that all four products performed differently in the six climate zones, although the RGD tended to perform better in wet climates than in dry climates. Alijanian et al. (2017) evaluated the performance of five RGD in eight climatic zones in Iran through correlation coefficient, root mean square error and relative error during the period 2003–2012. Their results showed that the performance of RGD varies with climate zones, with better performance in very hot and humid climates. The same conclusions were drawn for heavy rainfall (rainfall above the 90th percentile) for two RGD in China by Fang et al. (2019). In addition to the influence of climate on the performance of RGD, Fang et al. (2019) showed that topography also has a significant influence on heavy rainfall estimation, with correlation coefficients that decrease with altitude. These few examples show the advantages and limitations of the RGD in the regions studied, and the need to evaluate their performance for the Lesser and Greater Antilles because the climate dynamics of these islands have a range of concurrent interactions between mid-latitudes and tropical features at all spatial scales (Martinez et al., 2019).

In the Caribbean region, several studies have used RGD as baseline data to study spatial and temporal rainfall variability (Angeles et al., 2010; Jones et al., 2016; Jury, 2016), flood mapping (Bozza et al., 2016) and the dynamic mechanisms that determine the spatial and temporal patterns of the seasonal cycle (Martinez et al., 2019; Moron et al., 2016), but very few studies compared such databases with rainfall observations. in the Caribbean region, which including the Greater and Lesser Antilles. However, very few studies have evaluated their performance specifically in the Greater and Lesser Antilles. A first comparison between rainfall observations, reanalysis, satellite and coupled model datasets was performed by Jury (2009). The first part of the study aimed to evaluate in a qualitative

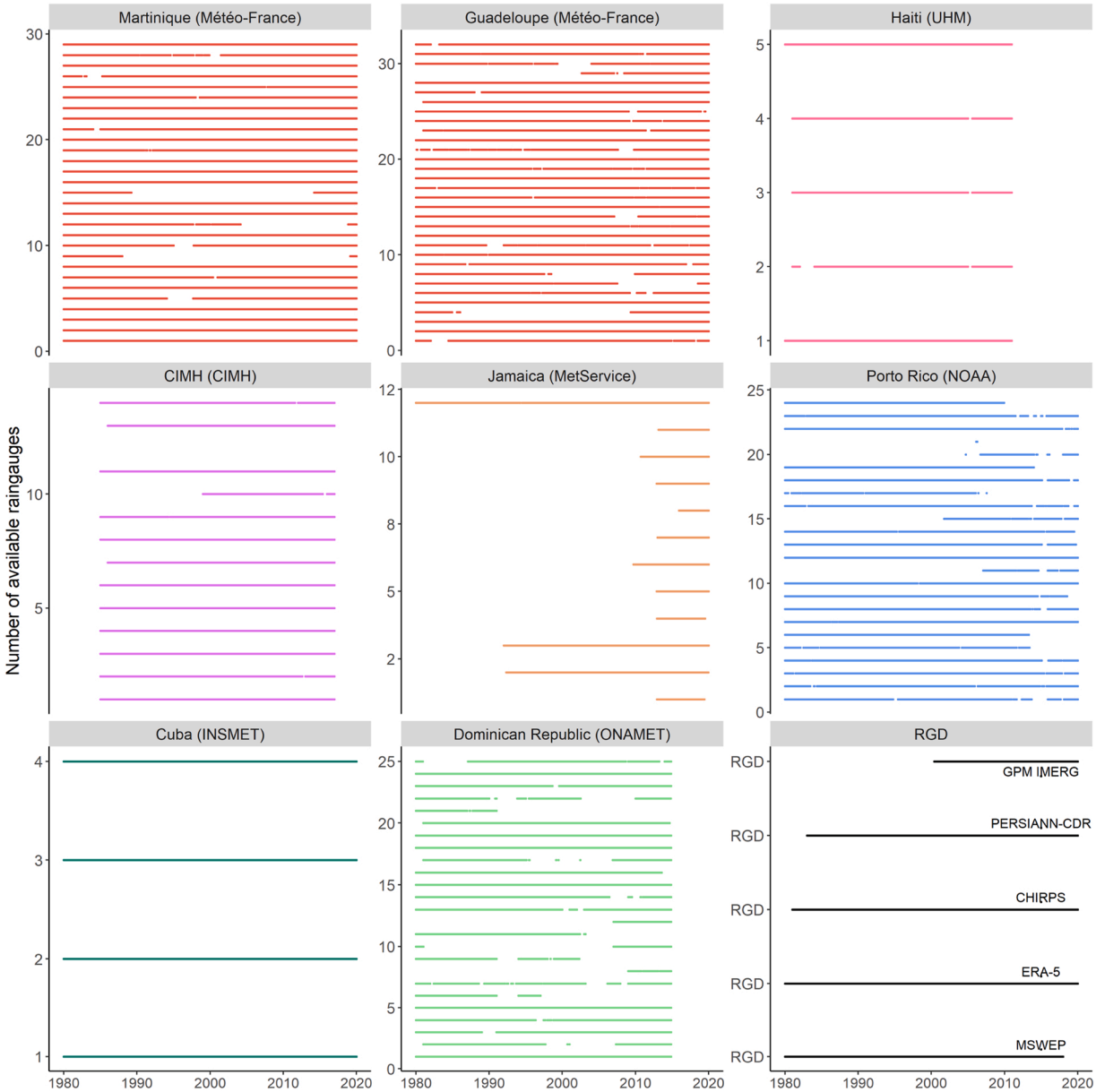

Fig. 2. Periods of data availability for each of the rain gauge databases used.

way the ability of RGD to capture several climatic features over the Caribbean region, and the second part of the study evaluated the ability of gridded rainfall to capture the annual rainfall cycle. More recently, a study evaluating the performance of 16 RGD on a monthly timescale was done by Centella-Artola et al. (2020) in the Caribbean. The results show that MSWEP is one of the best performing RGD, and ERA-5 performed best among the reanalysis products. Both the evaluations by Jury (2009) and Centella-Artola et al. (2020) were done on a monthly timescale. Nevertheless, using long (typically several decades) temporal series at the daily or sub-daily timestep is required for hydrological studies dedicated to heavy rainfall and flood statistics. The performance of these rainfall gridded datasets products varies from one timescale to another, and they tend to perform better on a monthly than a daily timescale (Sultana and Nasrollahi, 2018; Tan et al., 2015). In this context, this work aims to evaluate the general performance of five rainfall gridded datasets (RGD) available at the daily time step over the period 1980–2019 (MSWEP, CHIRPS, ERA-5, PERSIANN-CDR and GPM IMERG). These four RGD are chosen according to (i) their performance in the Greater and Lesser Antilles on a monthly timescale (Centella-Artola et al., 2020) and (ii) their availability on a daily timescale over several decades. To our knowledge, this is the first study on the evaluation of RGD in the Greater and Lesser Antilles on a daily timescale, aiming to highlight the qualities and shortcomings of RGD over these poorly instrumented islands. This paper is structured as follows: Section 2 presents the study area, Sections 3 and 4 present the data and methods used, Sections 5 and 6 present the results and discussion, and Section 7 presents conclusion to the

paper.

2. Study area

The study area, shown in Fig. 1, is the region between North America and South America and includes the islands that are surrounded by the Gulf of Mexico in the North-West, the Caribbean Sea in the South and the Atlantic Ocean in the East. These islands are often represented in two major groups: The Greater Antilles, grouping Cuba, Hispaniola, Jamaica and Puerto Rico and the Lesser Antilles, which is an island group located to the East and Southeast of the Caribbean Sea and composed of the islands of the Southern part of the Caribbean arc from Puerto Rico to South America.

The Greater Antilles has a bimodal annual rainfall cycle, with a first rainy season in May and a second rainy season between September and November. This bimodal annual rainfall cycle is influenced by the NASH (North Atlantic Subtropical High; Davis et al., 1997) and the CLLJ (Caribbean Low-Level Jet; Cook and Vizy, 2010). The Lesser Antilles has a unimodal annual rainfall cycle strongly influenced by the ITCZ (Intertropical Convergence Zone; Hastenrath, 2002), with peak rainfall in November.

The heavy rainfall in the Greater and Lesser Antilles, observed between September and November, is strongly influenced by tropical cyclones of the North Atlantic. 85 % of intense tropical cyclones originate in East African Waves (Agudelo et al., 2011; Thorncroft and Hodges, 2001) coupled with the Atlantic Warm Pool (area with sea temperatures greater than 28.5 °C; Wang and Enfield, 2003) and the Intertropical Convergence Zone.

Rainfall in the Greater and Lesser Antilles depends on dominant easterlies, topography, and land-sea interactions. The spatial pattern of rainfall in these islands is very inhomogeneous due to their complex topography (Cantet, 2017; Moron et al., 2015). Rainfall is relatively important (2 000–4 000 mm/year) in the higher elevations and windward parts (Smith et al., 2012). In contrast, annual rainfall can be as low as 500 mm/year in the leeward areas (Daly et al., 2003).

3. Rainfall data used

The rainfall data used in this study are classified into two categories: the rain gauge data that will be used as reference and the RGD (Rainfall Gridded Datasets). A short description of both types of rainfall dataset is provided below.

3.1. Rain gauge data

3.1.1. Presentation of the reference rain gauges

The set of 146 rainfall series that we will use in this study comes from several institutions: Météo-France, the Hydrometeorological Unit of Haiti (UHM), the Caribbean Institute for Meteorology and Hydrology (CIMH), the National Oceanic and Atmospheric Administration (NOAA), the Meteorological Service of Jamaica (MetService), the Meteorological Institute of the Republic of Cuba (InsMet) and the National Meteorological Office of the Dominican Republic (ONAMET). Fig. 2 presents the gaps in the data availability for each dataset.

3.1.2. Quality control of the reference rain gauges

Rain gauge data are used as reference data to evaluate the performance of RGD in the Greater and Lesser Antilles. These reference data can have considerable measurement errors (Sevruk et al., 2009; Viney and Bates, 2004), therefore, quality control is an essential step before evaluating the RGD. To identify and discard periods or rain gauges with significant measurement errors, we used a procedure with the following steps (this method is inspired by that of Beck et al., 2019):

a) Remove the rainy days with more than 1000 mm/d,
b) Remove months with more than 20 days of missing data,
c) Remove years with more than 200 days of missing data,
d) Remove stations with less than 5 years of data,
e) Test the uniformity of the data series from the annual sum of the stations by the method of cumulative residuals as described by Bois (1987). This method consists of plotting the cumulative residuals of the linear regression between a reference station and a station to be tested. The 90 % confidence intervals for the cumulative residuals of each year are plotted, to form a confidence ellipse inside which the curve of the cumulative residuals should remain. The reference station is a synthetic station formed by the median of the annual accumulations of all stations in the same country.

19 of 146 rain gauges were removed after quality control testing on reference data. Among the 127 rain gauges remaining, 27 are in Guadeloupe, 25 in Martinique, 21 in Dominican Republic, 5 in Haiti, 4 in Cuba, 10 in Jamaica, 22 in Puerto Rico and 13 in small islands where CIMH provided rain gauge data.

3.1.3. Independence of the rain gauges from the stations used for RGD development

Of the five RGD used in our analysis, three RGD (MSWEP, CHIRPS and PERSIANN-CDR) have been used rainfall products derived from rain gauges such as GPCC (Schneider et al., 2014), GSOD (https://www.ncei.noaa.gov/access/metadata/landing-page/bin/iso?id=gov.noaa.ncdc:C00516), GHCN (Menne et al., 2012) and GPCP (Adler et al., 2003), and two RGD (CHIRPS and MSWEP) have been used rain gauges directly. The rain gauges used by CHIRPS are form Mexico, Central America, South America and sub Saharan Africa

(Funk et al., 2015) and not from the Greater and the Lesser Antilles. However, Beck et al. (2019) have been used daily rainfall series form the Greater and the Lesser Antilles to calibrate MSWEP rainfall dataset. We excluded the 24 rain gauges (Figure A.2 in appendix) identified as positioned within a 1-km radius from rain gauges mentioned as used within the MSWEP V2.8 dataset to ensure the independence of the rain gauges from the stations used for RGD development. Among the 103 rain gauges remaining, 27 are in Guadeloupe, 22 in Martinique, 19 in Dominican Republic, 5 in Haiti, 2 in Cuba, 10 in Jamaica, 6 in Puerto Rico and 12 in small islands where CIMH provided rain gauge data.

3.2. RGD (Rainfall Gridded Datasets)

3.2.1. Precipitation Estimation from Remotely Sensed Information using Artificial Neural Networks–Climate Data Record (PERSIANN-CDR)

PERSIANN-CDR is a multi-satellite product that provides daily precipitation estimates with a spatial resolution of 0.25° from 1983 onwards (Ashouri et al., 2015). The PERSIANN artificial neural model is pre-trained with NCEP (National Centers for Environmental Prediction) stage IV hourly precipitation radar data. Then, PERSIANN-CDR is generated by the PERSIANN algorithm using GridSat-B1 infrared data Knapp (2008)). The final product is adjusted with the monthly GPCP (Global Precipitation Climatology Project) product to ensure that both datasets are consistent on a monthly scale.

3.2.2. Climate Hazards Group Infrared Precipitation with Station data (CHIRPS)

CHIRPS precipitation estimates (version 2) are available from 1981 onwards with a spatial and temporal resolution of 0.05°/24 h (Funk et al., 2015). This database uses monthly precipitation climatology CHPClim (Climate Hazards Group Precipitation Climatology), quasi-global geostationary thermal infrared satellite observations, Tropical Rainfall Measuring Mission's (TRMM) 3B42 product, atmospheric model rainfall fields from NOAA CFS (Climate Forecast System), and precipitation observations from different sources, including national or regional meteorological services. The CHIRPS production requires two steps. First, pentad (five-day) rainfall estimates are created from CCD (Cold Cloud Duration) which are obtained from regression models, and calibrated by using TRMM 3B42 pentad precipitation; these estimates are expressed as a percentage of normal precipitation by dividing the estimated values for regression models by their long-term averages (this outcome is names CHIRP). Then, in-situ observation from stations are blended with CHIRP data in order to produce CHIRPS.

3.2.3. Multi-Source Weighted-Ensemble Precipitation (MSWEP)

The second version of MSWEP, as described by Beck et al. (2017) is a global gridded dataset for the period 1979–2017 with a spatiotemporal resolution of 0.1°/3 h. This dataset is derived by merging rainfall estimates based on rain gauges coming from different databases: [WorldClim (Fick and Hijmans, 2017), GHCN-D (Menne et al., 2012), GSOD (https://data.noaa.gov), and national databases from different country], different SRE: [CMORPH (Joyce et al., 2004), GridSat (Knapp et al., 2011), GSMaP (Ushio et al., 2009), and TMPA 3B42RT (Huffman et al., 2007)] and reanalysis: [ERA-Interim (Dee et al., 2011) and JRA-55 (Kobayashi et al., 2015)].

To build MSWEP, Beck et al. (2019) was evaluated the performance of the gridded datasets using the correlation coefficient of the gridded data with the 3-day mean rainfall data. Next, the data were merged via weighted averaging using the interpolated weight maps deduced from the correlation coefficients. The biases of the merged data are corrected by a multiplicative approach used by Vila et al. (2009) to preserve the sub-daily rainfall distribution.

3.2.4. ERA-5

We use the fifth generation of the atmospheric global climate reanalysis ERA-5 available from 1980 onwards with a spatiotemporal resolution of 0.25°/1 h (Hersbach et al., 2020). ERA-5 is produced by the European Centre for Medium-Range Weather Forecasts (ECMWF). This new reanalysis replaces the ERA-Interim reanalysis that started in 2006. ERA-5 benefits from decades of developments in the dynamics of data assimilation models and combines them with observations of wind, pressure, temperature, precipitation and humidity from several satellites and from observations near the earth's surface and over the oceans, from upper air soundings and from atmospheric measurements from aircraft instruments. This is based on the hybrid 4D-Var data assimilation method using the Cy41r2 cycle of the Integrated Forecast System (IFS) Cy41r2 (Hersbach and De Rosnay, 2018).

3.2.5. NASA Global Precipitation Measurement (GPM) Integrated Multi-satellitE Retrievals for GPM (IMERG)

The GPM IMERG was launched in February 2014 as the successor to TRMM, to provide the next generation of global precipitation products. It consists of one Core Observatory and approximately 10 constellation satellites. The Core Observatory carries a Ku/Ka-band dual-frequency precipitation radar and a multi-channel GPM IMERG microwave imager, extending the measurement range of TRMM instruments. GPM IMERG provides three levels of precipitation-related products. The level-3 products are produced with the IMERG algorithm, which intercalibrates and merges precipitation estimates from all constellation microwave sensors, microwave-calibrated infrared satellite estimates, and monthly gauge precipitation data (Hou et al., 2014). The GPM IMERG products, available from 2000 onwards, offer a relatively fine spatial resolution of 0.1° × 0.1° and high temporal resolution of 30 min. The GPM IMERG Day 1 Final Run V6 data is used in this study. The Final Run product introduces GPCC rainfall dataset (Schneider et al., 2014) for bias correction, generally considered to be more accurate results than the near real-time products (Early and Late Run), and is thus widely used in hydrology and climate researches (Huffman et al., 2015).

Table A.1 (in appendix) briefly lists the main characteristics of the selected gridded rainfall data – PERSIANN-CDR, CHIRPS, MSWEP, ERA-5 and GPM IMERG.

4. Methodology

In this section, we describe the methodology designed to evaluate the performance of RGD in the Greater and Lesser Antilles. Four of the used RGD are available from 1980 (PERSIANN-CDR, CHIRPS, MSWEP and ERA-5), and GPM IMERG is available from 2000. GPM IMERG is a RGD widely used in hydrological applications (Li et al., 2021; Pradhan et al., 2021; Wang et al., 2022) and has thus being used in this study despite its shorter temporal extension. Thus, we evaluated the performance of four RGD (MSWEP, ERA-5, CHIRPS and PERSIANN-CDR) over the 1980–2019 period and all five RGD over the 2000–2019 period. First, the method used to compare RGD grid points and rain gauges temporal series is presented (subsection 4.1). Then, the different performance measures calculated are listed (subsection 4.2).

4.1. Comparison between RGD grid points and rain gauges temporal series

4.1.1. Point-to-pixel analysis

A point-to-pixel analysis was applied to compare the time series of the reference rain gauge stations (i.e. the points) with the corresponding grid cell values (i.e. the pixels). This approach has been chosen over the pixel-to-pixel methodology (Saemian et al., 2021) given the sparse rain gauges density over the studied region. Thus, the application of a pixel-to-pixel methodology requires to have a gridded reference dataset or to spatially interpolate reference rain gauges data.

In the Lesser Antilles, particularly in the Martinique and Guadeloupe French Islands (cf. Figure A.3 in appendix), more than one rain gauge is counted on the same RGD pixel. For each RGD pixel containing more than one rain gauges, an area-weighted average of the considered rain gauge series has been performed using the Thiessen polygons (e.g. Liu et al., 2015; Tang et al., 2020).

4.1.2. RGD upscaling

The four RGD considered have different spatial resolutions. The point-to-pixel analysis has been performed (i) to the original RGD resolution, and also (ii) at a similar resolution of 0.25°, which is the resolution of the ERA-5 and PERSIANN-CDR coarser RGD considered. Thus, an upscaling of the CHIRPS, and MSWEP datasets has been performed to a new spatial resolution of 0.25° by using bilinear interpolation (Baez-Villanueva et al., 2018).

4.1.3. Use of two different rain gauges sets

The MSWEP RGD has been produced considering different ground datasets, including several rain gauges (see subsection 3.1.3). Thus, this bias-corrected dataset is expected to better perform than the RGD that do not use rain gauge stations (e.g. Baez-Villanueva et al., 2018). To ensure the independence of the rain gauge stations used as reference in our study and those used during the RGD construction, we calculated the performances of the RGD on two different rain gauges sets. First, 103 rain gauges are considered excluding the 24 rain gauges identified as positioned within a 1-km radius from rain gauges mentioned as used within the MSWEP V2.8 datasets. Then, all the 127 rain gauges are considered. The excluded rain gauges are identified in the Figure A.2 in appendix.

4.2. Evaluation of the RGD performances

The RGD were evaluated along four characteristics:

a) General performance.
b) Reproduction of wet and dry days.
c) Reproduction of rainfall seasonality.
d) Estimation of heavy rainfall.

4.2.1. General performances of the RGD

4.2.1.1. Performances at the daily time steps. The general performance of the RGD are evaluated at the daily time-step by five statistical metrics:

a) the root mean square error (RMSE [mm/d]),
b) the correlation coefficient (R [-]),
c) the α coefficient (α [-]): ratio of the standard deviation of the RGD to the standard deviation of the observations,
d) the β coefficient (β [-]), ratio of the mean of the RGD to the observations,
e) the Kling and Gupta Efficiency score (KGE [-], Gupta et al., 2009).

The KGE score is widely used in hydrology in order to compare observations with model simulations (e.g. Arciniega-Esparza et al., 2022; Mathevet et al., 2020), and is also used the context of RGD comparison with rain gauges series (e.g. Baez-Villanueva et al., 2018; Centella-Artola et al., 2020; Saemian et al., 2021). The KGE is a combination of the R, β and α coefficients, and thus evaluates the general performance of the RGD in reproducing rainfall in the Greater and the Lesser Antilles. The optimal values of the α, β coefficients

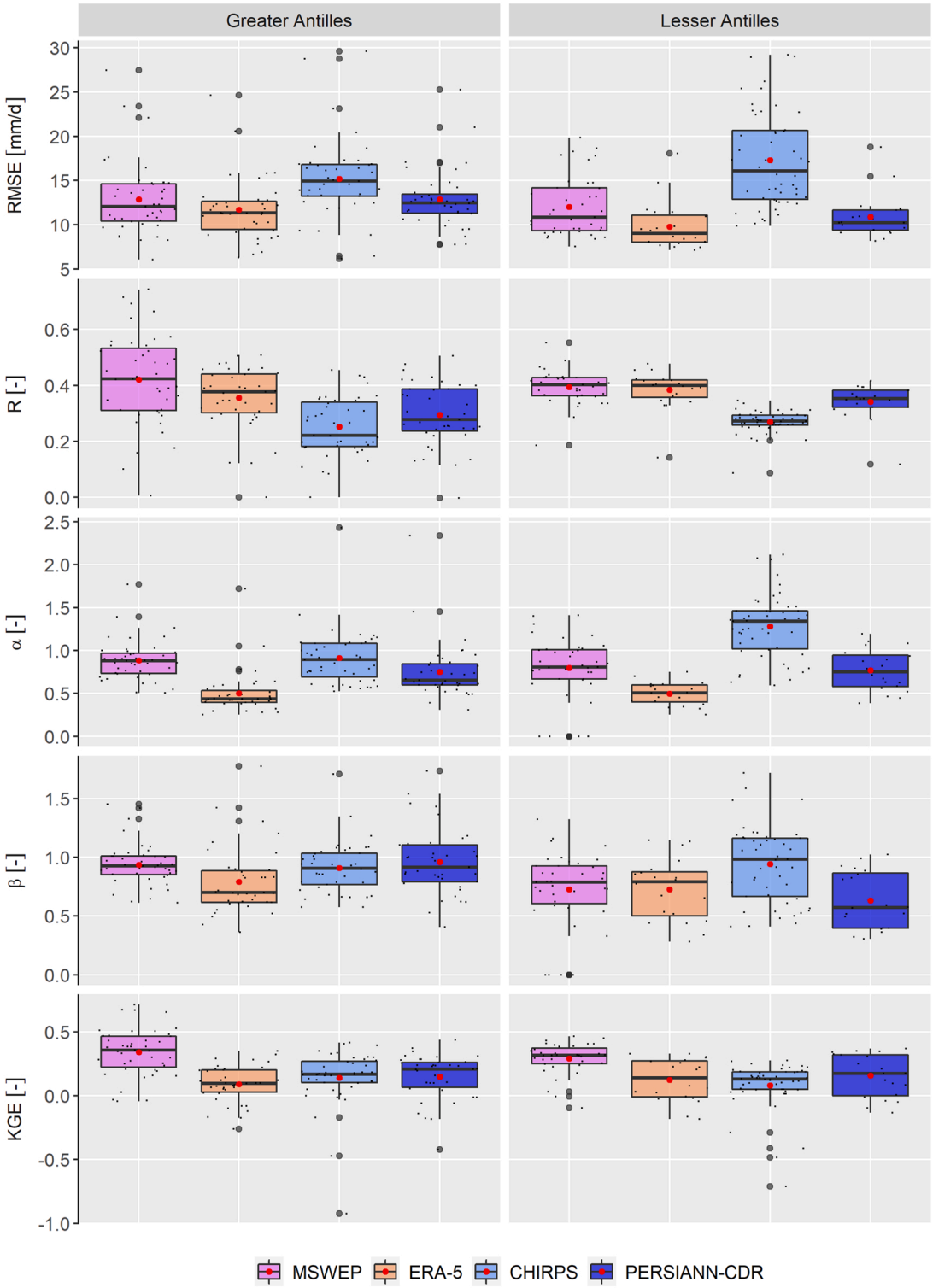

Fig. 3. General performance of the RGD on a daily timescale via 5 statistical metrics in the Greater Antilles and Lesser Antilles. These boxplots offer a summary of the distribution of the scores calculated on each of the 103 considered rain gauges: the center line indicates the median, the red point indicates the mean, the edges of the box are the 1st quartile and the 3rd quartile, the ends of the box define a threshold that cannot exceed 1.5 times the interquartile range, and the black points, if any, are points that are outside the threshold of the box.

and of the KGE criteria are 1. The correlation coefficient is used to evaluate the linear relationship between the RGD and the rain gauges, the results vary between − 1 and + 1, where − 1 indicates a perfect negative correlation while + 1 indicates a perfect positive correlation. The α coefficient evaluates the dispersion of the RGD compared to the observed data. The β coefficient evaluates the bias of the RGD by measuring the average tendency of the RGD values to overestimate ($\beta > 1$) or underestimate ($\beta < 1$). The root mean square error is used as a measure of the average absolute error; an optimal value for RMSE is 0 mm/d.

4.2.1.2. Performances at the monthly and annual time steps. General performances of the RGD are also evaluated at the monthly and annual timesteps, by estimating R, α and KGE on monthly and annual time series (Kuentz et al., 2015). Note that β has the same value on these different timescales.

4.2.2. Rainfall detection

Three categorical statistics criteria are used to evaluate the capacity for RGD to detect wet and dry days. There are four possible cases (Mashingia et al., 2014): i) the RGD detects rainfall that is really observed; ii) the RGD detects rainfall that is not observed; iii) the RGD does not detect rainfall that is observed; and iv) the RGD and rain gauge do not detect any rainfall. Based on these cases, the following categorical statistics are evaluated:

a) The probability of detecting rainfall (POD [-]),
b) The false alarm rate (FAR [-]),
c) The critical success index (CSI [-]).

The probability of detection measures the capacity of the RGD to correctly detect the rainfall observed, the results are between 0 and 1 (optimal value). The false alarm rate measures the proportion of days in which the RGD measures rainfall that was not observed by the rain gauges, results are between 0 (optimal value) and 1. The critical success index illustrates the fraction of observed rain that was correctly detected by the RGD, the optimal value of the critical success index is 1 (Alijanian et al., 2017). Table A.2 (in appendix) lists the statistical metrics used to evaluate the RGD over the Lesser and the Greater Antilles.

4.2.3. Rainfall seasonality

Annual rainfall cycles are calculated with the 15-day aggregated rainfall data for the 103 reference rain gauges and on the RGD pixels corresponding to these reference data. Below the 15-day aggregation, the annual rainfall patterns are noisy and of little interest. The finest timescale relevant to present the annual rainfall pattern is the 15-day aggregation. The result is averaged over the Greater and the Lesser Antilles to highlight the annual rainfall pattern and to assess the ability of the RGD to reproduce the rainfall seasonality in the area study.

4.2.4. Heavy rainfall statistics

The ratios of the 90th and 99th rainfall percentiles and the maximum annual rainfall of each reference rain gauge to the corresponding RGD are calculated to estimate the ability of the RGD to assess heavy rainfall in the Greater and Lesser Antilles. A ratio greater than 1 indicates an overestimation of RGD and a ratio below 1 indicates an underestimation of RGD. Lastly, the summary statistics such as average, maximum and standard deviation were calculated for selected rainfall percentiles of the rainfall datasets.

5. Results

5.1. Evaluation of the RGD performances over 1980–2019

5.1.1. RGD general performance on a daily timescale

Fig. 3 summarizes the performance of the RGD in estimating daily rainfall in the Greater and Lesser Antilles through the KGE criterion and its components (correlation coefficient, dispersion and bias) and the mean square error, using the 103 considered rain gauges. Overall, the performance over the Greater and Lesser Antilles are not significantly different. MSWEP is the most correlated with the reference data with a correlation coefficient of 0.5 in the Greater Antilles and slightly less in the Lesser Antilles. MSWEP has a good dispersion and a low bias, with α and β coefficients close to 1. These relatively good values of R, α and β coefficients combine to produce a relatively good KGE for MSWEP, with values between 0.45 and 0.5 in the Greater and Lesser Antilles. ERA-5 is the second most correlated RGD with the reference data with correlation coefficients between 0.35 and 0.4 but that, the dispersion around the mean value of ERA-5 is low (α near to 0.5) and a priori the estimates of ERA-5 are relatively uniform and are unable to capture heavy rainfall well, as shown in Fig. 8 and Fig. 9. ERA-5 underestimates the reference data with biases (β) between 0.65 and 0.75. This weakness in the dispersion around the mean value and underestimation of the reference rainfall makes ERA-5 the worst performing RGD, with KGE between 0.1 and 0.15. PERSIANN-CDR has a better KGE score than CHIRPS in the Lesser Antilles, mainly due to a better correlation of PERSIANN-CDR compared to CHIRPS. However, in the Greater Antilles, the R, α and β coefficients and thus the KGE scores of PERSIANN-CDR and CHIRPS are similar. Overall, the performance of CHIRPS in the Lesser and Greater Antilles is impaired by its low correlation coefficient with the reference data, but the lack of performance of ERA-5 is influenced by their low dispersion around the mean value (α near to 0.5). The RMSE coefficient is relatively low for ERA-5 and PERSIANN-CDR and is about 11 mm/d. In contrast, the RMSE coefficient is very high for CHIRPS and is about 17 mm/d.

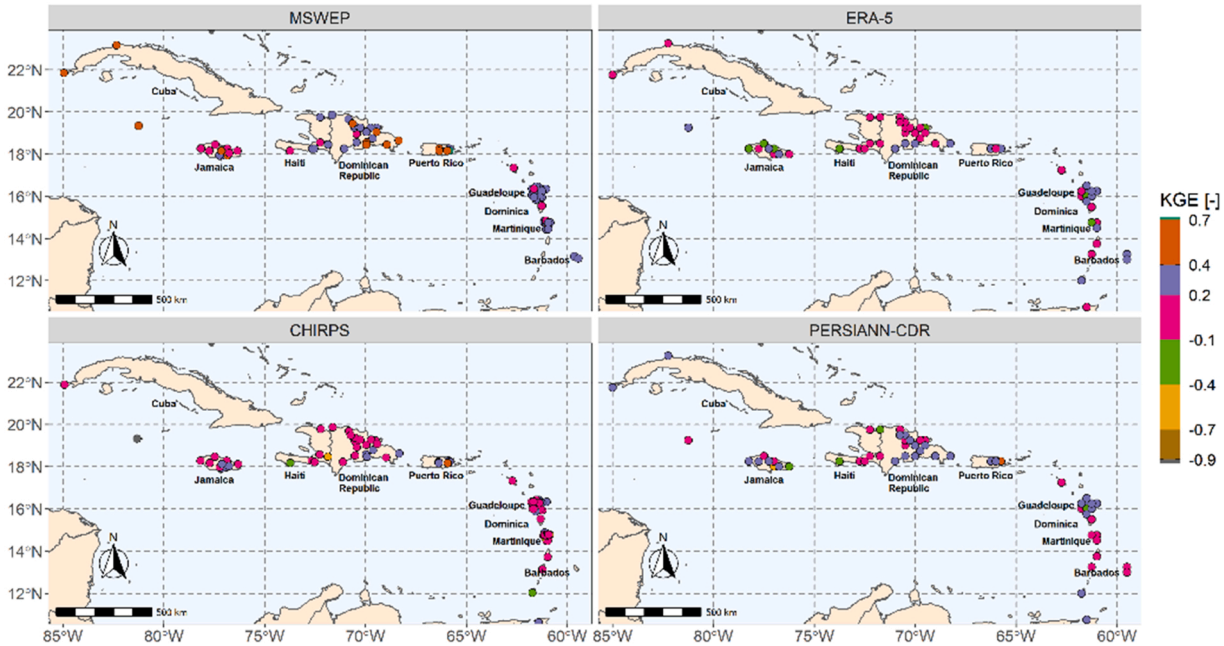

Fig. 4. Spatial distribution of KGE scores for 4 RGD in the Greater and Lesser Antilles.

Fig. 4 shows a spatial representation of the performance results of the four RGD via the KGE statistical metric. In general, the KGE score tends to be relatively high in the Eastern Greater Antilles (Dominican Republic and Puerto Rico) in particular in Puerto Rico and in the North of the Lesser Antilles including Guadeloupe and the KGE score is relatively low in the West of the Greater Antilles, notably in Haiti and Jamaica, and in the North of the Lesser Antilles including Martinique. MSWEP shows the same spatial pattern in the Greater Antilles but the KGE scores are almost uniform in the Lesser Antilles and have no particular spatial pattern.

5.1.2. RGD rainfall detection capacity evaluation indices

The ability of the RGD to identify wet and dry days is presented in Fig. 5.

ERA-5 then MSWEP have a good capacity to reproduce the rainy days observed on the ground for the Lesser and Greater Antilles (POD > 0.9 for ERA-5 and POD > 0.75 for MSWEP, that is, on all the wet days recorded by the rain gauge, 90 % were detected by ERA-5 % and 75 % by MSWEP). The false alarm rate is on average 0.5 in the Greater Antilles and 0.25 in the Lesser Antilles: out of all the wet days detected by an RGD, 50 % were not observed in the rain gauges of the Greater Antilles and 25 % in the Lesser Antilles. The fraction of rainfall observed and correctly detected by the RGD, represented by the CSI coefficient, was 0.5 for MSWEP and ERA-5 in the Greater Antilles and 0.65–0.7 for MSWEP and ERA-5 in the Lesser Antilles, and in the range of 0.25–0.30 for CHIRPS and PERSIANN. In summary, ERA-5 is the best performing RGD to identify wet and dry days before MSWEP with a very high POD and a similar CSI although FAR of ERA-5 is higher than MSWEP. In contrast, CHIRPS is the least efficient RGD to identify wet and dry days with low POD and CSI. These results are very important as these RGD may be used to calculate extreme climate indices such as the annual number of wet days above a certain threshold, annual number of wet days, or the maximum number of consecutive dry days and therefore the results obtained should be adjusted accordingly.

5.1.3. RGD general performance on daily, monthly and annual timescales

In this section, we present, in addition to the daily timescale evaluated in Sections 5.1.1 and 5.1.2, the ability of the RGD to estimate rainfall on monthly and annual timescales using the KGE criterion and their R, α and β components. The biases β is not shown in Fig. 6 because it is constant on daily, monthly and annual timescales. The dispersion α changes slightly on daily, monthly, and annual scales, with ERA-5 showing low dispersion around the mean value (relatively uniform rainfall) at all three timescales. Only the correlation coefficient affects the performance of the RGD at the three temporal scales studied. All RGD correlate very well with the reference rainfall data on a monthly scale with correlation coefficient values that reach, on average, 0.75 for MSWEP in the Greater Antilles and for all RGD in the Lesser Antilles. The correlation coefficients on an annual scale are slightly worse than those on a monthly scale but significantly better than the daily scale correlation coefficients (R>0.7 at the monthly time scale and R<0.5 at the daily time scale; see Fig. 6). Although the correlation coefficients of all RGD are better on monthly and annual scales, the KGE scores of ERA-5 in the Greater Antilles and ERA-5 and PERSIANN-CDR in the Lesser Antilles are significantly reduced because of their biases and their low α coefficient at daily, monthly and annual scales.

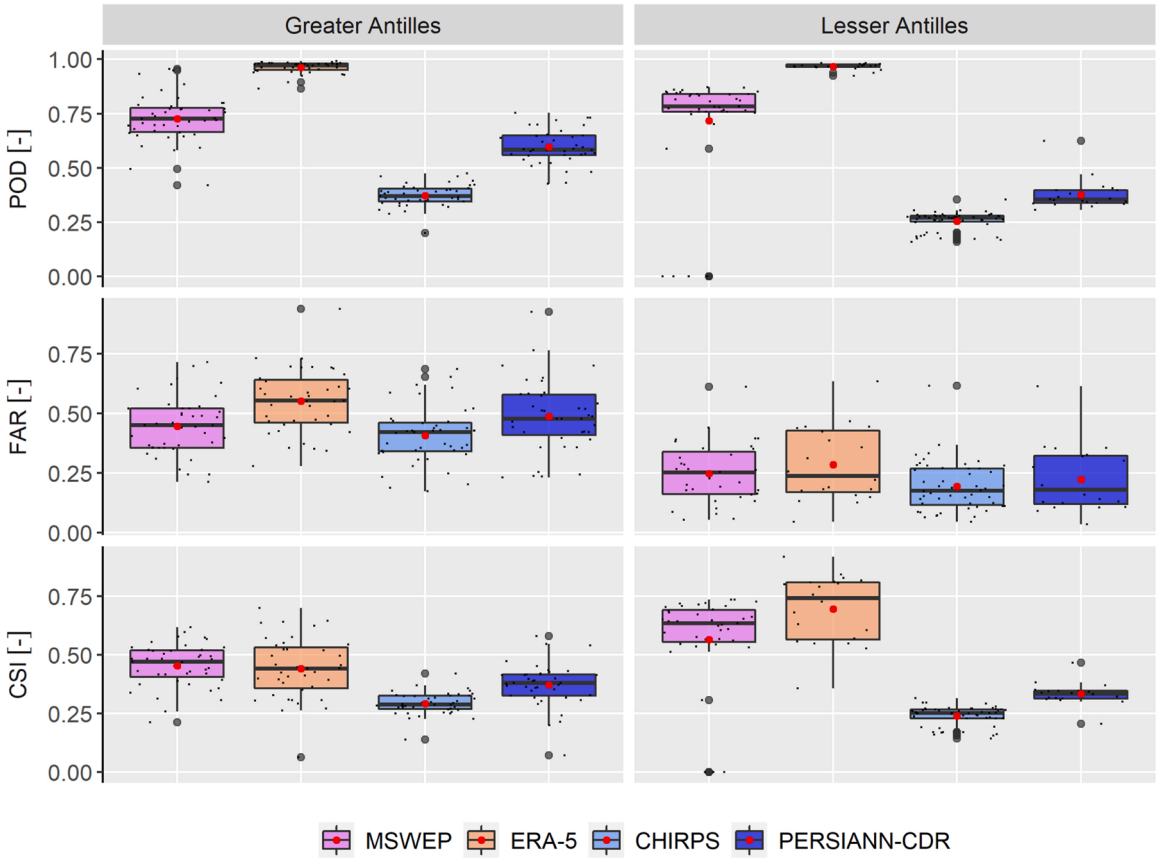

Fig. 5. RGD capacity to indicate dry and wet days with 3 categorical statistical metrics in the Greater Antilles and Lesser Antilles. These boxplots offer a summary of the distribution of the scores calculated on each of the 103 considered rain gauges: the center line indicates the median, the red point indicates the mean, the edges of the rectangle are the 1st quartile and the 3rd quartile, the ends of the lines define a threshold that cannot exceed 1.5 times the interquartile range, and the black points, when they exist, are points that are outside the threshold of the box.

5.1.4. The annual rainfall cycle

The reference rainfall series as well as the corresponding RGD pixels were aggregated over a 15-day period, and the annual average rainfall cycle was calculated for each aggregated data series. Then, the annual rainfall cycles were averaged for the Greater and Lesser Antilles (see Fig. 7). The results show that the average annual rainfall cycle in the Greater Antilles is divided into 4 seasons with two rainfall peaks during the year. Winter dry season (WDS) from late November to mid-March with an average rainfall of 3 mm/d, early rainy season (ERS) from mid-March to mid-May with a peak rainfall of about 7 mm/d, mid-summer drought (MSD) from mid-May to early August which is a less rainy season interspersed between the two heavy rainy seasons with a rainfall of a little over 4 mm/d and late rainy season (LRS) from early August to late November with an average rainfall of 7 mm/d. These four seasons are also observed in the Lesser Antilles, however, with the MSD season being wetter than the ERS season. As a result, the Lesser Antilles has an increasing rainfall from WDS to reach a peak of about 8 mm/d in late October to early November. All the RGD have well captured the general pattern of the mean annual cycle well, with a bimodal precipitation cycle (a peak of rainfall in mid-May and a late rainy period from August to November) in the Greater Antilles and of the unimodal cycle in the Lesser Antilles. In the Greater Antilles, the rainfall amounts of the MSWEP, CHIRPS and PERSIANN-CDR from mid-May to early November are in very good agreement with the reference data, but these RGD underestimate the rainfall from November to early May. All RGD strongly underestimate rainfall in the Lesser Antilles except CHIPRS, which reproduces the annual rainfall cycle very well. ERA-5 and PERSIANN-CDR capture the amplitude of the rainfall in the Lesser Antilles very poorly.

5.1.5. Heavy rainfall performance indices

In this section, we will present the ability of the studied RGD to estimate heavy rainfall accurately, by studying their 90th and 99th percentile rainfall and their maximum annual rainfall.

Fig. 8 gives a spatial representation of the ratios, r, of 90th percentiles of the RGD estimates to the reference data and thus shows the areas where the 90th percentile rainfall is overestimated or underestimated by the RGD. Areas of underestimation ($r < 1$) of the reference data are represented by dots and areas of overestimation ($r > 1$) are represented by triangles. Overall, the RGD tend to slightly underestimate the 90th percentile rainfall in the study area and especially in the Lesser Antilles and the Eastern part of the

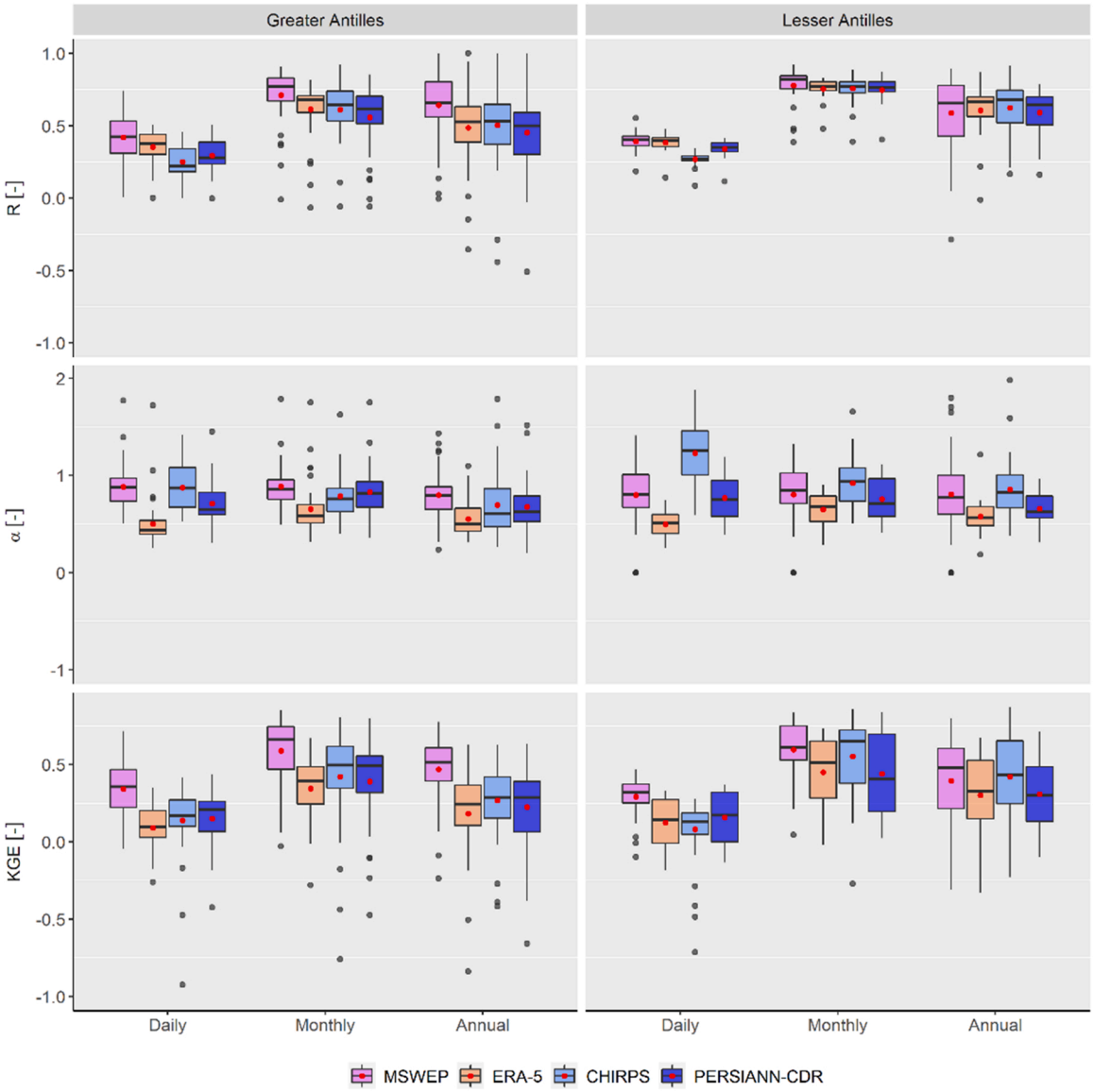

Fig. 6. RGD performance on daily, monthly and annual timescales using the KGE criteria in the Greater Antilles and Lesser Antilles. These boxplots offer a summary of the distribution of the scores calculated on each of the 103 considered rain gauges: the center line indicates the median, the red point indicates the mean, the edges of the rectangle are the 1st quartile and the 3rd quartile, the ends of the lines define a threshold that cannot exceed 1.5 times the interquartile range, and the black points, when they exist, are points that are outside the threshold of the box.

Greater Antilles, but all the RGD systematically overestimate the reference data in the north of Haiti and south-east of Cuba, and sometimes in Jamaica. Although RGD tend to underestimate the 90th percentile rainfall, MSWEP and CHIRPS have a good ability to estimate the 90th percentile rainfall (r close to 1) in the eastern part of the Greater Antilles and in the northern part of the Lesser Antilles. This spatial variability of heavy rainfall is fairly well measured by CHIRPS with, however, an overestimation of the 90th percentile rainfall in the Lesser Antilles and a little less well by MSWEP with an underestimation of the heavy rainfall percentiles. ERA-5 and, to a lesser extent, PERSIANN-CDR strongly underestimate heavy rainfall percentiles and are unable to represent them spatially over the Greater and Lesser Antilles.

The results of the RGD performance in estimating heavy rainfall are summarized in Fig. 9. The gray horizontal line delineates the area where the RGD overestimate the reference percentiles (area above the line) from the area where the RGD underestimate the reference percentiles (area below the line). RGD are generally better at estimating heavy rainfall in the Greater Antilles than in the Lesser Antilles. CHIRPS and MSWEP perform well in estimating heavy rainfall percentiles in the Greater Antilles and somewhat less well in the Lesser Antilles. In general, all RGD tend to underestimate the 90th and 99th rainfall percentiles and the maximum annual rainfall in the Greater and Lesser Antilles except CHIRPS which overestimates these heavy rainfall percentiles in the Lesser Antilles.

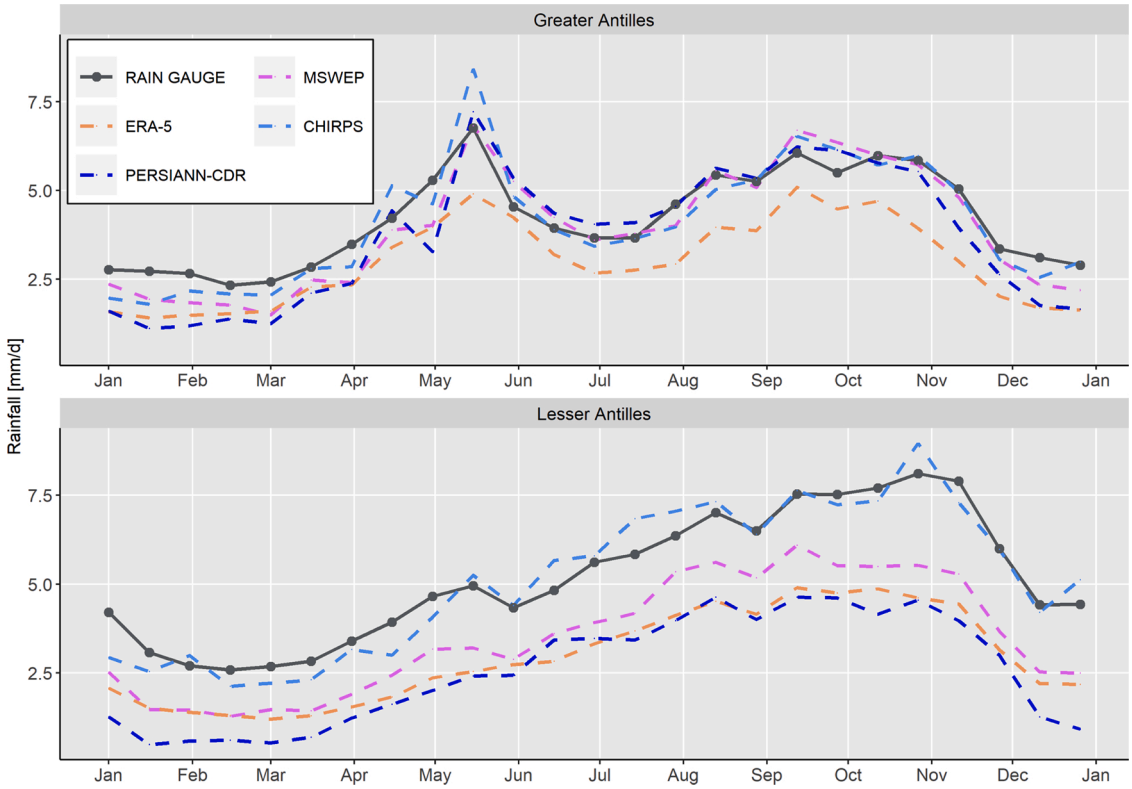

Fig. 7. Reference data and RGD annual rainfall cycle in the Greater Antilles and Lesser Antilles (1980–2019 period).

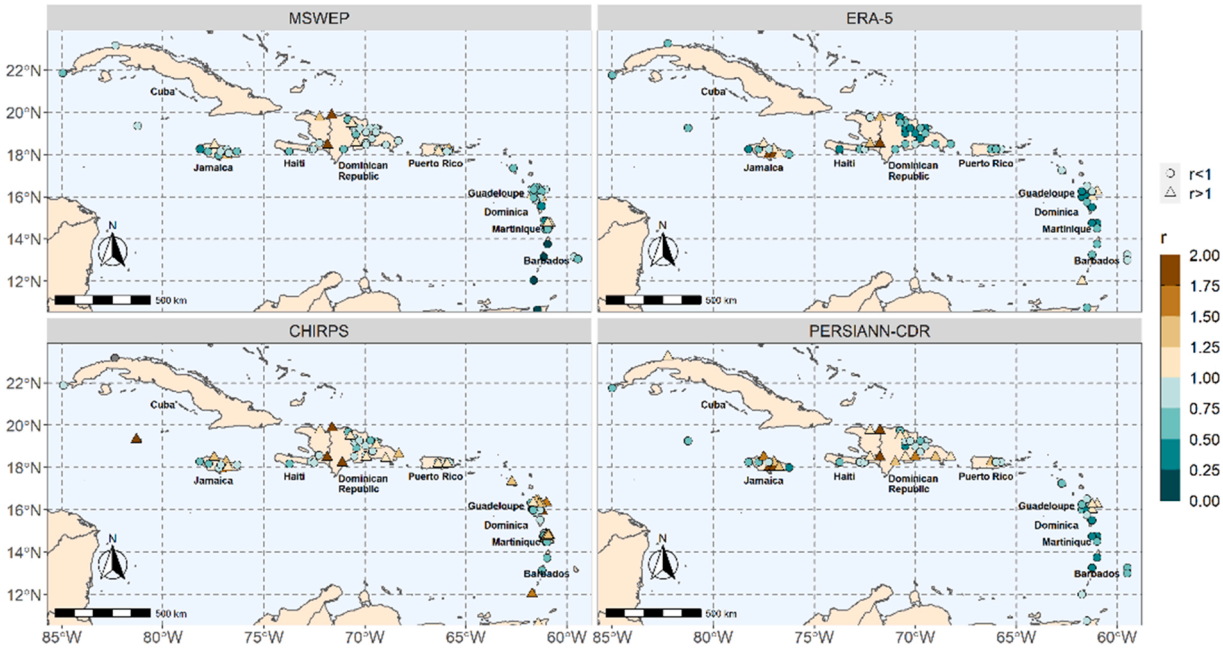

Fig. 8. Spatial distribution of the ratios (r) of 90th rainfall percentile of RGD to reference data in the Greater and the Lesser Antilles. Underestimation is represented by circles and overestimation is represented by triangles.

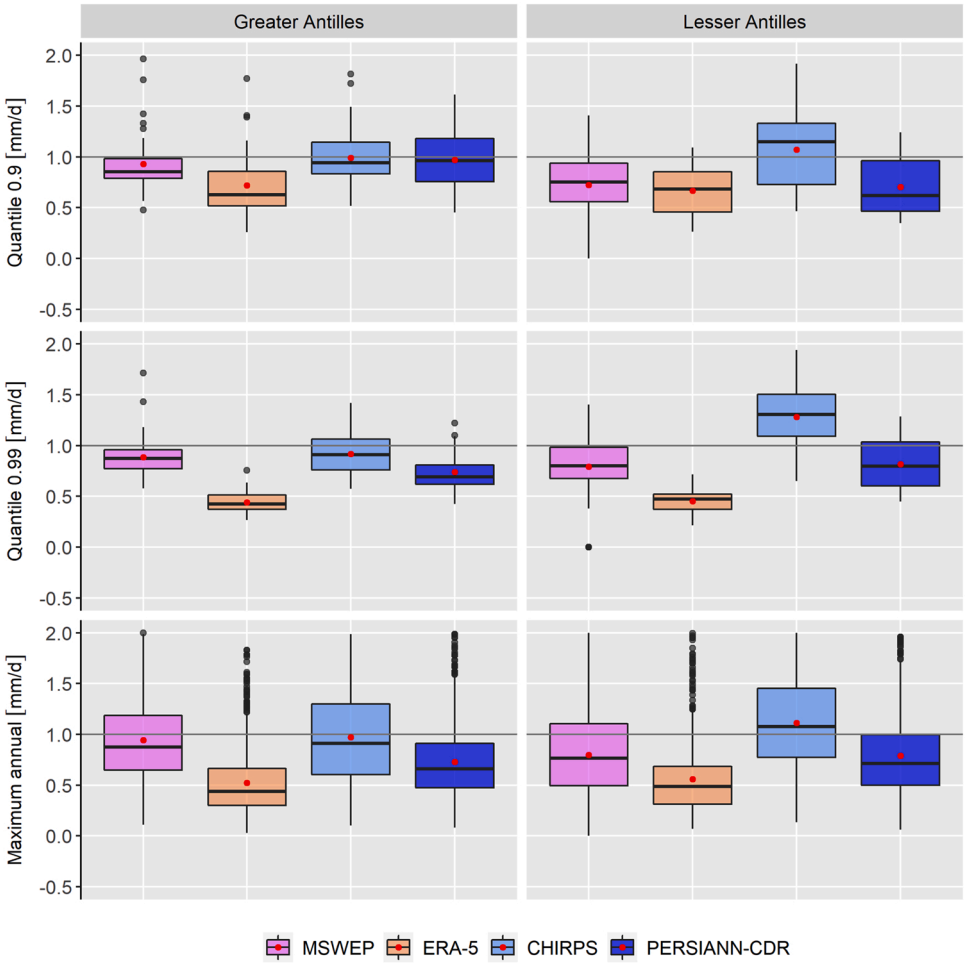

Fig. 9. Ratio of 90th and 99th rainfall percentiles and annual maximum rainfall of the RGD to the reference rainfall data in the Greater Antilles and Lesser Antilles. These boxplots offer a summary of the distribution of the scores calculated on each of the 103 considered rain gauges: the center line indicates the median, the red point indicates the mean, the edges of the rectangle are the 1st quartile and the 3rd quartile, the ends of the lines define a threshold that cannot exceed 1.5 times the interquartile range, and the black points, when they exist, are points that are outside the threshold of the box.

ERA-5 underestimates by half the percentiles of heavy rainfall in the Greater and Lesser Antilles and is the least efficient of the four RGD.

The 5 %, 25 %, 50 %, 75 % and 95 % rainfall percentiles are calculated for the 103 considered rain gauges and corresponding RGD pixels in the Greater and Lesser Antilles. The mean, maximum and standard deviation values of each rainfall database used are presented in Table A.3 in appendix. The results show that on average more than 75 % of the days during our study period had rainfall less than 5 mm/d and these low rainfall events are well captured by ERA-5 and PERSIANN-CDR. In contrast, CHIRPS, MSWEP and PERSIANN-CDR tend to capture the heavy rainfall percentiles, with CHIRPS overestimating heavy rainfall percentiles and MSWEP and PERSIANN-CDR underestimating them. Although PERSIANN-CDR gives good estimates of heavy rainfall percentile values, it strongly underestimates the maximum values.

5.1.6. Performance of original and upscaled RGD

The statistical metrics described in the methodology section are computed for the RGD with their original spatial resolution (see subsections 4.1.2 and 4.2.1) and additionally computed for a shared spatial resolution upscaled to 0.25°. We present in Fig. 10 the results for two quantitative metrics (the RMSE and the KGE) and the three qualitative metrics (POD, FAR and CSI) for the original and upscaled MSWEP and CHIRPS RGD (the original ERA-5 and PERSIANN-RGD are already at 0.25° so they are not upscaled). A decrease of the RMSE values is observed for the upscaled RGD, which is much more pronounced for CHIRPS, especially in the Lesser Antilles. In general, we observe a decrease in the KGE metric for the upscaled RGD, except for CHIRPS in the Lesser Antilles. Overall, the upscaled RGD have a better ability to detect rainy days and dry days, represented by a higher POD and CSI, despite the fact that the FAR increased for CHIRPS in the Greater Antilles.

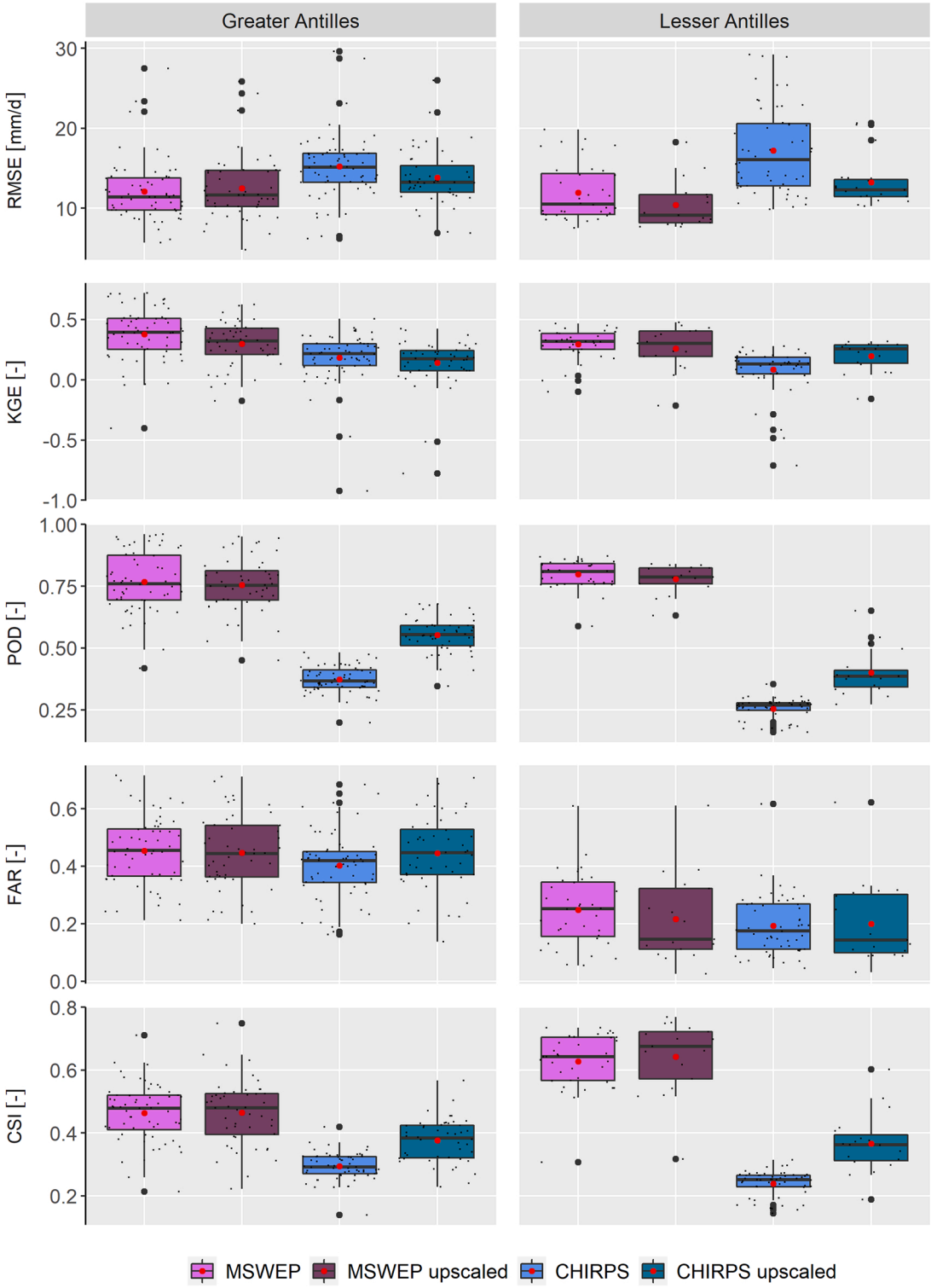

Fig. 10. Performances of the original and upscaled MSWEP and CHIRPS RGD.

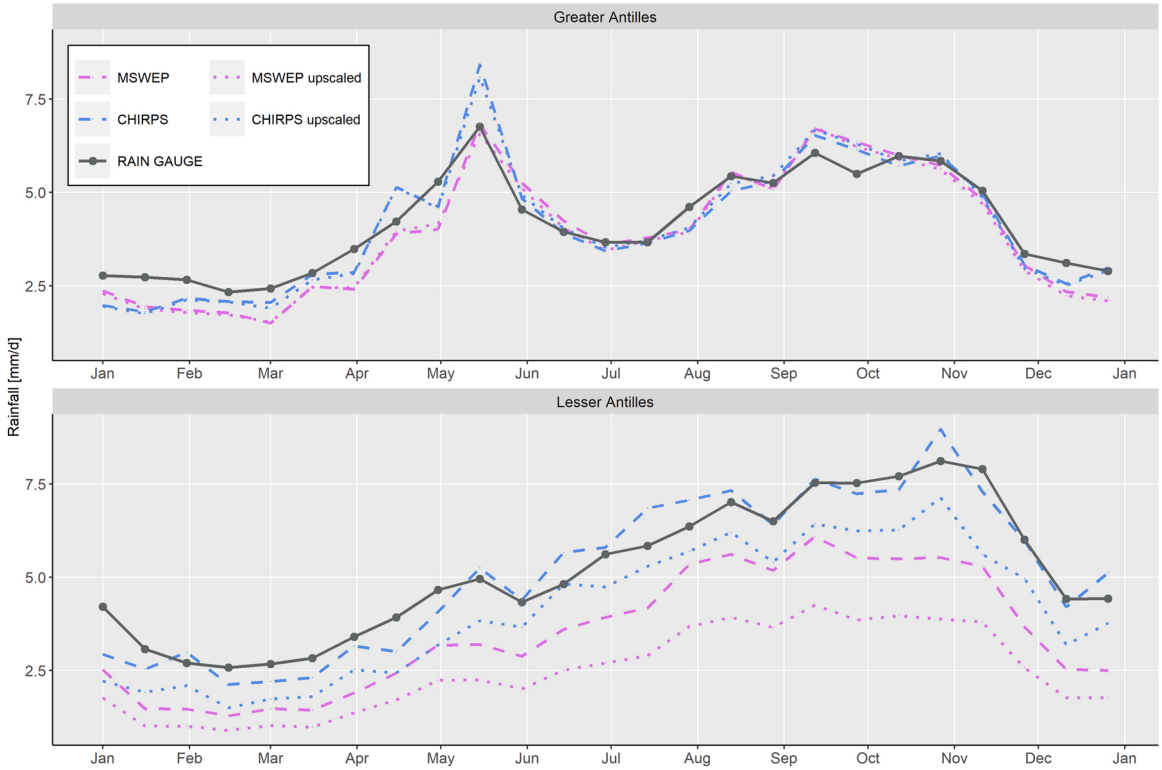

Fig. 11. Reference data and RGD annual rainfall cycle in the Greater Antilles and Lesser Antilles for the original RGD (left) and the upscaled RGD (right).

Fig. 11 shows the rainfall regime pattern of the original and upscaled RGD. The patterns obtained at the 0.25° resolution are generally similar to these obtained at the original spatial resolution, with an overall underestimation of rainfall for the upscaled RGD. The rainfall is strongly underestimated, particularly in the rainy season (September to November) in the Lesser Antilles. Although the RGD underestimate the rainfall, they correctly capture the rainfall regime (Fig. 11) for the two spatial resolutions. These results show that the rainfall regime pattern is more sensitive to the spatial scale variation of the RGD in the Lesser Antilles than in the Greater Antilles.

5.1.7. Performance of three rain gauges sets

The performance of the four RGD is evaluated using the sets of rain gauges described in Section 4.1.3. The first subset (subset 1, see Fig. 12) consists of 103 rain gauges excluding the 24 rain gauges used in MSWEP, the second subset (subset 2) consists of only the 24 rain gauges used in MSWEP, and the third subset consists of all the rain gauges (subset 1 + 2). The results are presented in Fig. 12 for the KGE criterion, which synthesizes the performance of three statistical metrics and is a good tool to evaluate the overall performance of the RGD (the results of all 5 quantitative statistical metrics for subsets 1 were presented in Fig. 3, while the results for subsets 1 + 2 are presented in the Appendix in Figure A.1). Clearly, the performance of MSWEP is much better than the other three RGD for subset 2 (Fig. 12), because these rain gauges are used to calibrate MSWEP. The ranks of performance of the RGD with subset 1 and subset 1 + 2 are similar, with a somewhat better performance of MSWEP with subset 1 + 2.

5.2. Evaluation of the RGD performances over 2000–2019

Fig. 13 presents the performance of the five RGD over 2000–2019 using five statistical metrics. The results shown in Fig. 13 do not show any significant difference in terms of MSWEP, CHIRPS, PERSIANN-CDR and ERA-5 RGD performance over the two time periods studied. GPM IMERG has difficulty to quantify rainfall volume in our study area, with the highest RMSE in the Greater Antilles, negative KGE in both the Greater Antilles and Lesser Antilles, and poorly represents heavy rainfall (not shown) although its performance is better than ERA-5 and PERSIANN-CDR. However, GPM IMERG has a good ability to detect rainy and dry days, with POD and CSI scores better than CHIRPS in the Greater Antilles and CHIRPS and PERSIANN-CDR in the Lesser Antilles.

GPM IMERG has difficulty representing the rainfall regime in the Greater and Lesser Antilles, as shown in Fig. 14. The May rainfall peaks are captured late (around June and sometimes early July) by GPM IMERG. November rainfall peaks in the Lesser Antilles are captured early (late August to early October) by GPM IMERG. In addition, GPM IMERG underestimates the rainfall pattern in the winter dry season (WDS) and overestimates the rainfall regime from May to November.

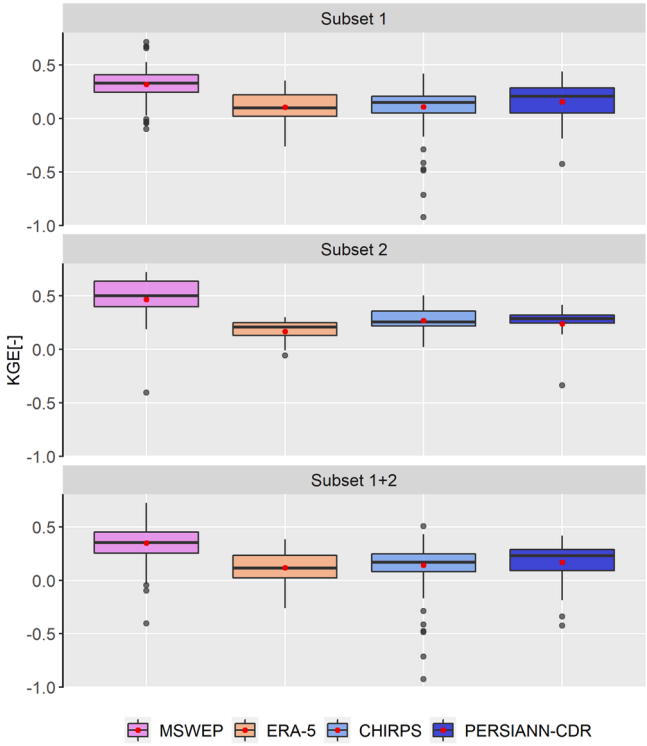

Fig. 12. KGE scores obtained by 4 RGD over both Greater and Lesser Antilles considering 3 subsets of rain gauges: subset 1 is composed by 103 rain gauges, subsets 2 consists in 24 rain gauges used in MSWEP, and subset 3 consists in all the 127 rain gauges.

6. Discussion

6.1. Comparison of RGD performances

The performance of the RGD over the studied region reflects the philosophy behind their design. MSWEP was designed for operational research in hydrology to improve our understanding of hydrological processes and enhance hydrological model performance (Beck et al., 2019). Thus, MSWEP has been produced by merging gridded rainfall data and daily rainfall data. Therefore, MSWEP performs well in most of the statistical metrics considered. CHIRPS is designed for monitoring extremes, which is why CHIRPS gives good estimates of heavy rainfall percentiles over the studied region. The performance of PERSIANN-CDR is poor over our study area. This poor performance of PERSIANN-CDR might be due to the data used to construct precipitation datasets. PERSIANN-CDR has used an algorithm based on artificial neural networks with trained by the stage IV radar data but this radar data itself is biased (Habib et al., 2009; Sharif et al., 2020). In addition PERSIANN-CDR used mainly infrared (IR) data that provide a measure of cloud top brightness temperature, which correlates with the probability of cloud precipitation (Brochart and Andréassian, 2014). But the performance of an IR-based algorithm is less accurate for some types of cloud: warm rain clouds and cold high cirrus, non-raining clouds (Ashouri et al., 2015) Reanalysis products are designed to study climate variability on a large spatio-temporal scale and have wide application in atmospheric sciences. This explains the good ability of ERA − 5 to detect rainfall occurrences (high POD) but due to its too coarse spatial resolution, ERA-5 underestimates the rainfall amplitude in our study area.

The poor performance of GPM IMERG can be explained because it is a purely satellite-based RGD and does not use reference rain gauges to calibrate its estimates. Pradhan et al. (2022) have reviewed the performance of GPM IMERG at the global scale and show that GPM IMERG does not perform well to represent heavy and light rainfall, especially at the daily and sub-daily scales. Despite its limitations, the fine spatio-temporal resolution of GPM IMERG and its improvement with each new version (Pradhan et al., 2022) reveals a promising path for current and future applications.

6.2. Are RGD limitations over Lesser and Greater Antilles site-specific?

Although MSWEP is the best performing RGD, the general performances obtained over the Greater and Lesser Antilles are lower than performances obtained by MSWEP over other regions: in Southeast Asia (Tang et al., 2019), Iran (Alijanian et al., 2017) and Austria (Sharifi et al., 2019), correlation coefficients obtained by comparing MSWEP and rain gauges at the daily timestep are generally greater than 0.75, while these correlation coefficients are less than 0.6 in the Caribbean. This can be explained by the fact that most satellite products have difficulty observing local convection systems in the Caribbean islands (Jury, 2009).

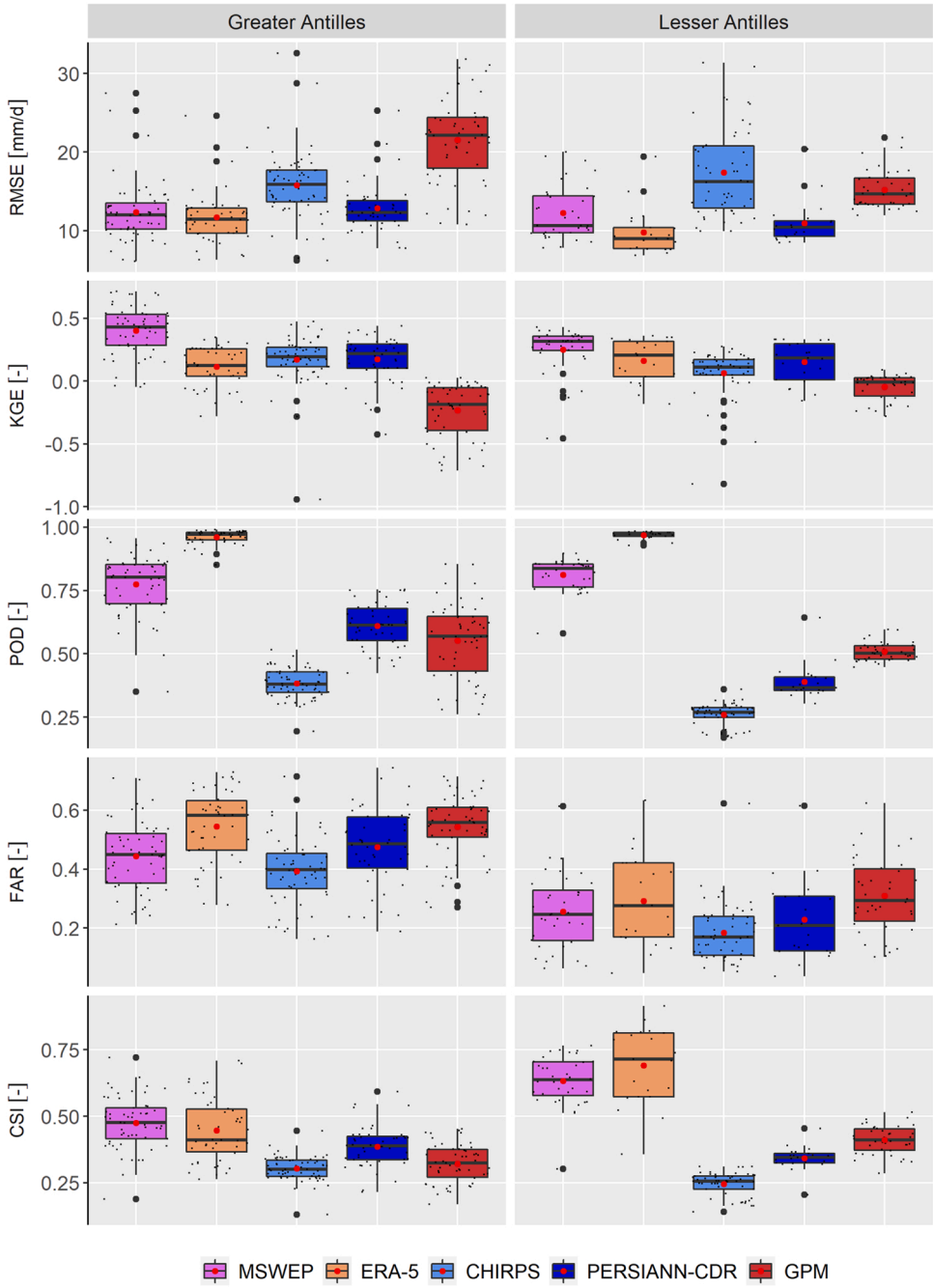

Fig. 13. Performance of the five RGD over 2000–2019.

The winter dry season (WDS; Fig. 7) in the Greater Antilles is underestimated by all four RGD while the other three seasons are well reproduced. These results corroborate the work of Brochart and Andréassian (2014) who showed that low rainfall tends to be underestimated by RGD in French Guyana.

The four RGD overestimate the rainfall percentiles in the area between the western part of Hispaniola and eastern Cuba (Fig. 8). This corroborates the result of Jury (2009) showing that remotely sensed rainfall products fail to capture the low rainfall area between Haiti, Cuba and Jamaica, due to the mountainous terrain rising to 2000 m in a northwest-southeast axis extending for 200 km, creating a significant wind and rain shadow towards Jamaica and Cuba.

The topography is very complex and influences the spatial pattern of rainfall. However, the rain gauges used in our study are mostly located in low-lying areas and this is of little relevance to study the relationship between topography and rainfall. The use of the Digital Terrain Model (DEM) in the Greater and Lesser Antilles to study the spatial variability of rainfall and to evaluate the performance of the

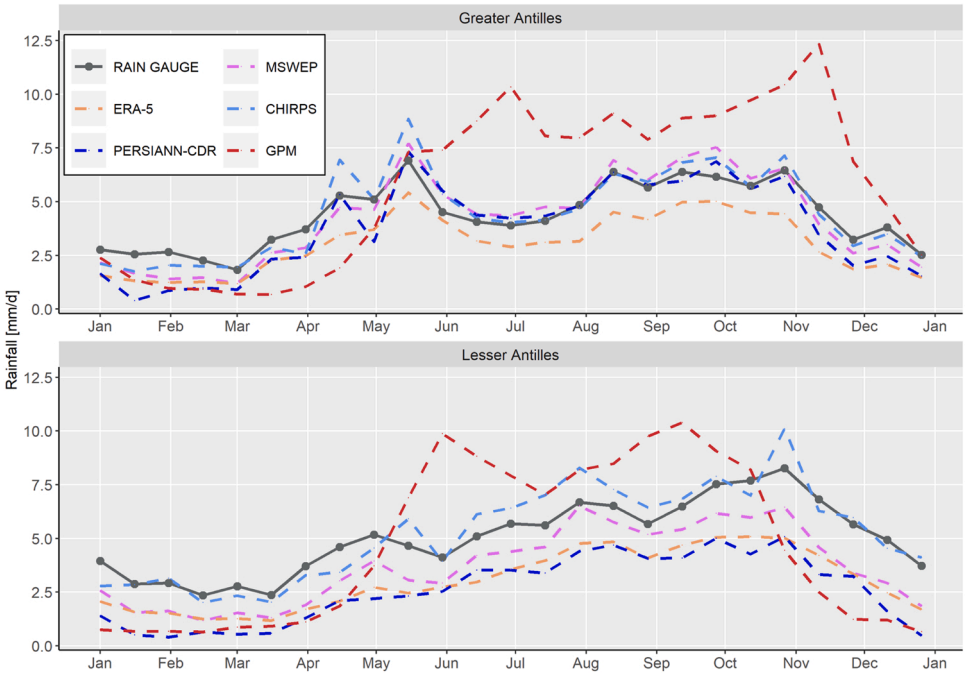

Fig. 14. Reference data and RGD annual rainfall cycle in the Greater Antilles and Lesser Antilles (2000–2019 period).

RGD in relation to the topography is an interesting perspective.

6.3. Limitation of the point-to pixel comparison

The point-to-pixel comparison allows to compare the point data of the rain gauges to the area data of the RGD. The comparison of the performances of the original and upscaled RGD allows to evaluate the impact of the spatial resolution of the RGD on their performance and thus to evaluate the limit of the point-to-pixel approach. There was no clear trend in the impact of the spatial resolution of the RGD on their performance. For the two quantitative metrics used, we observed a decrease in KGE (except for CHIRPS in the Lesser Antilles), and an improvement in RMSE for the upscaled RGD. The RMSE strongly penalizes errors on heavy rainfall, but the RGD upscaled tend to smooth heavy rainfall and therefore, the RMSE is less penalizing with the RGD upscaled. This may explain the better RMSE score for the upscaled RGD. Therefore, caution should be used when evaluating the performance of RGD using RMSE (Baez-Villanueva et al., 2018) as the results may not reflect the real performance of RGD. The ability of RGD to capture both rainy and dry days is improved for upscaled RGD. This can be explained by the RGD being averaged over a larger area and therefore having a higher number of rainy days than the original RGD. This could either increase the number of days of rainfall detected by the RGD and rain gauges and/or decrease the number of days of rainfall detected by the rain gauges and not by the RGD and therefore increase the POD and/or CSI.

The underestimation of rainfall cycle pattern by the RGD, particularly in the Lesser Antilles (Fig. 11), can be explained by the spatial resolution of the RGD, which is too coarse compared to the surface area of the Lesser Antilles islands (e.g. 1128 km^2 for Martinique). Indeed, the largest spatial resolution of the RGD is 0.25° (more than 650 km^2) which represents more than half the area of Martinique. The RGD rainfall is therefore averaged over too large an area and does not adequately capture the rainfall peaks and its spatial variability in this region.

6.4. Uncertainty of the reference rain gauge observations?

The spatial patterns of the KGE score show that KGE scores are systematically higher in some countries (Puerto Rico and Martinique) than in others (Haiti and Jamaica for example) for all RGD. The results may well show a good performance of the RGD in the East of the Greater Antilles and the North of the Lesser Antilles. However, this result should be taken with caution as we have assumed that the observed rainfall series is the reference, without taking into account uncertainty of these reference series. Moreover, the best KGE scores are obtained for countries whose meteorological services have well documented and good quality reference data such as NOAA and Météo-France. Thus, there is a possibility that the spatial pattern of KGE scores may reflect countries with good quality reference data.

In our study, the effect of using a large number of reference rain gauges in the Lesser Antilles and a small number of reference rain gauges in the Greater Antilles was not evaluated, particularly on the underestimation of the rainfall cycle in the Lesser Antilles.

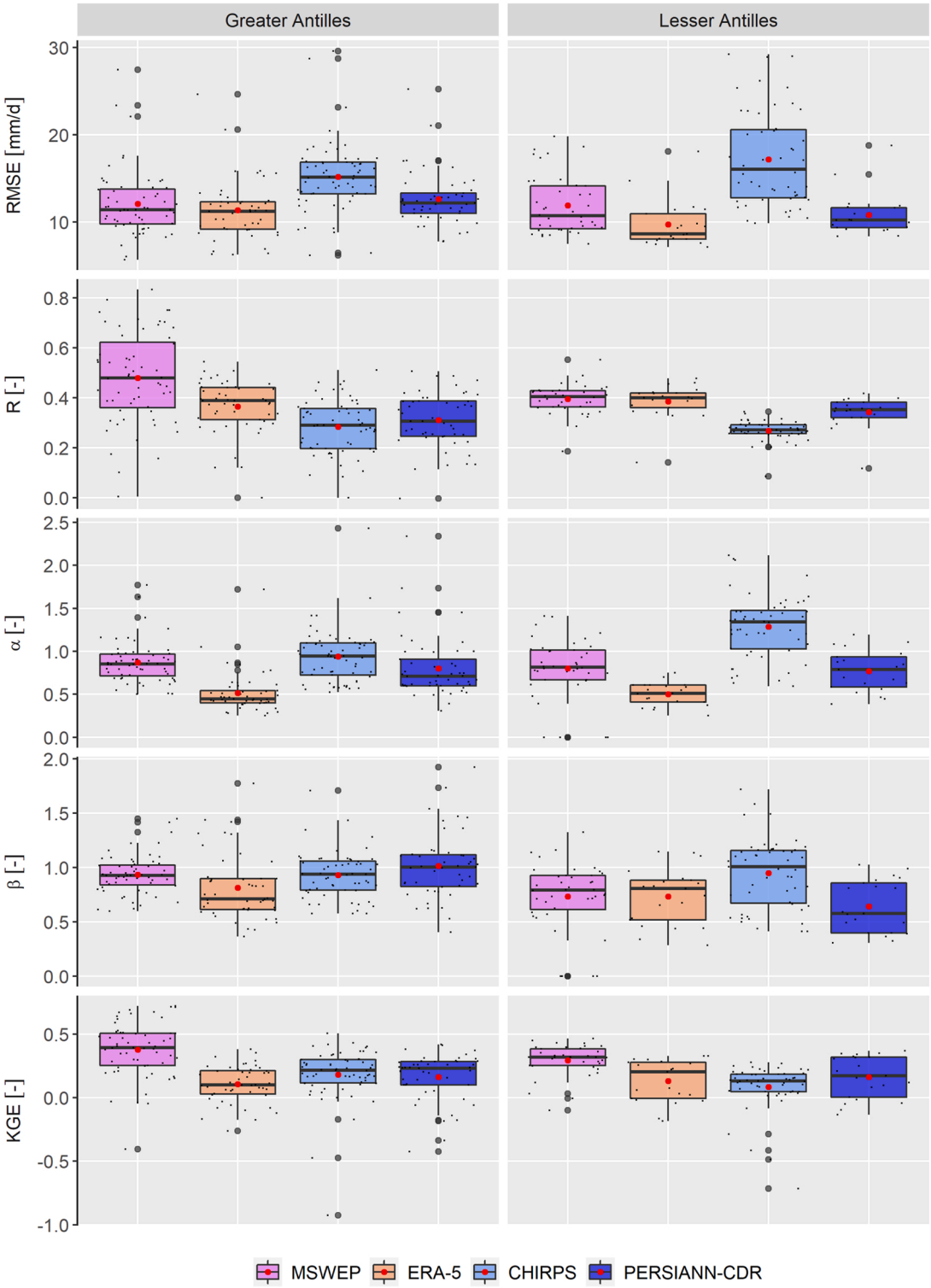

Fig. A1. General performance of the RGD on a daily timescale via 5 statistical metrics in the Greater Antilles and Lesser Antilles. These boxplots offer a summary of the distribution of the scores calculated on each of the all 127 rain gauges: the center line indicates the median, the red point indicates the mean, the edges of the box are the 1st quartile and the 3rd quartile, the ends of the box define a threshold that cannot exceed 1.5.

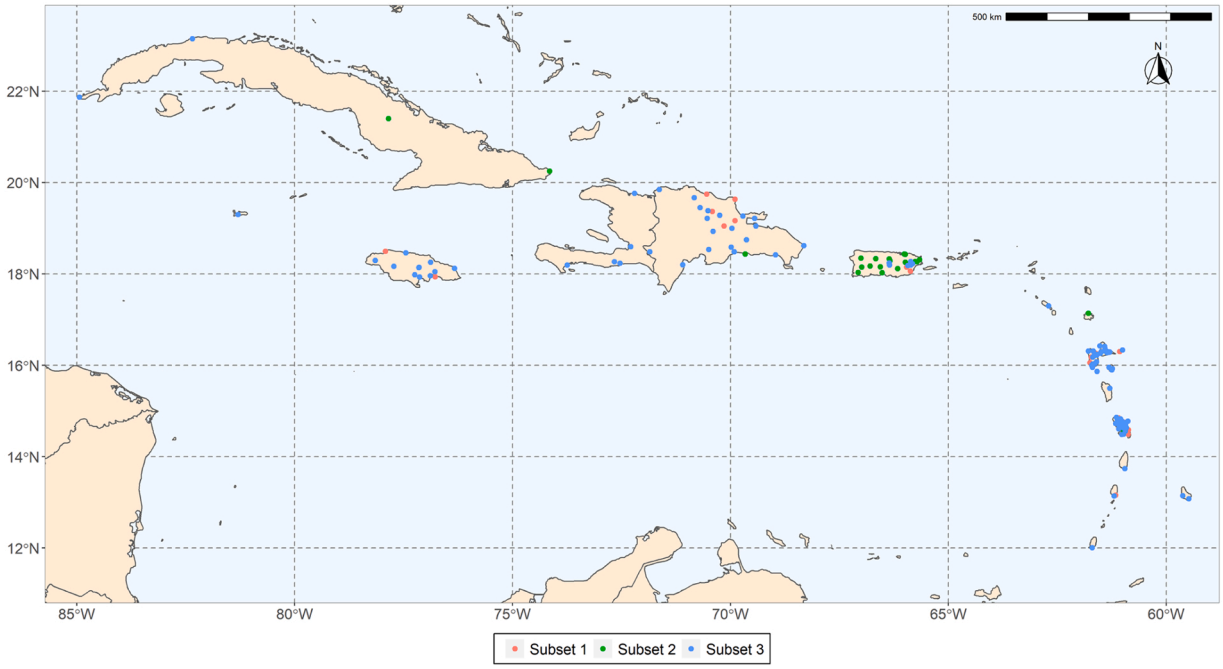

Fig. A2. - Position of the rain gauges constituting the three subsets: The first subset consists of 103 rain gauges excluding the 24 rain gauges used in MSWEP, the second subset (subset 2) consists of only the 24 rain gauges used in MSWEP, and the third subset consists of all the rain gauges (subset 1 + 2).

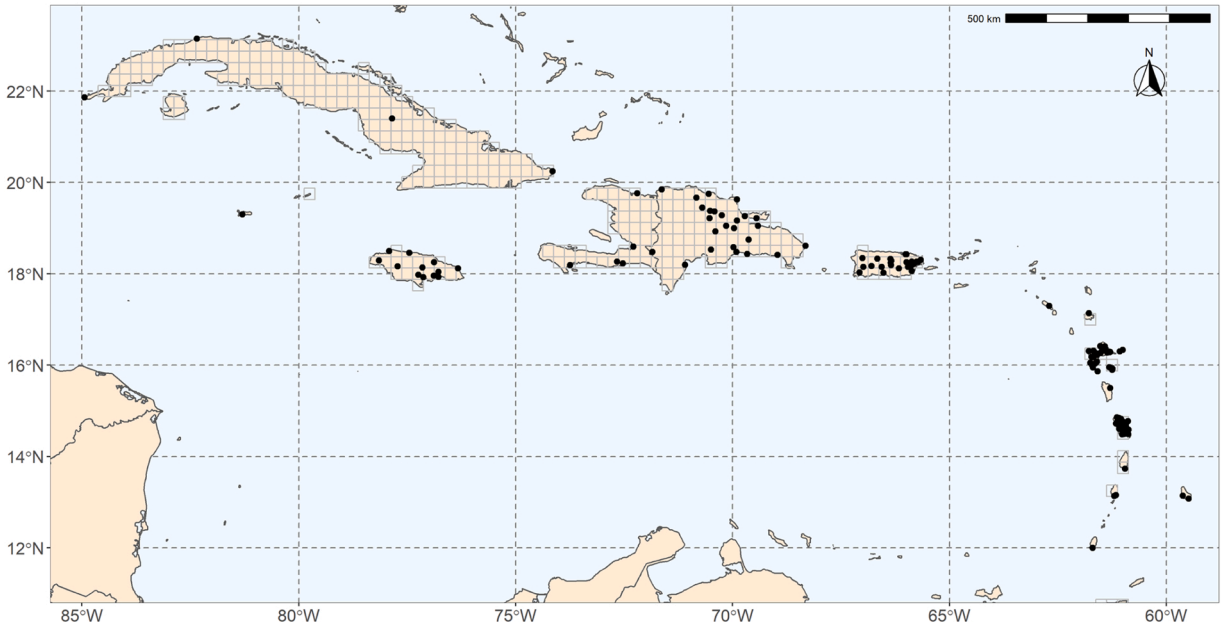

Fig. A3. All the 127 rain gauges and the PERSIANN-CDR grid cells.

Nevertheless, Centella-Artola et al. (2020) considered a larger number of rain gauges over the Greater Antilles and showed that RGD underestimate the rainfall cycle in the Lesser Antilles, particularly during the rainy season (September to November).

7. Conclusion

In this study, the performance of five Rainfall Gridded Datasets (RGD) - namely MSWEP, CHIRPS, PERSIANN-CDR, ERA-5 and GPM

Table A1
Summary of the selected satellite products.

Satellite product	Temporal resolution	Spatial Resolution	Period
PERSIANN-CDR	Daily	0.25°	1983-present
CHIRPS	Daily	0.05°	1981-present
MSWEP	3 hourly	0.10°	1979–2017
ERA-5	1 hourly	0.25°	1979-present
GPM IMERG	Half-hour	0.10°	2000 - present

Table A2
List of statistical metrics used to evaluate RGD performance. X_i represents rain gauge data, $\overline{X}$ represents mean rain gauge data, Y_i represents RGD data, $\overline{Y}$ represents mean RGD data, n represents the data length available, a represents rainfall detected both by the rain gauge and the RGD, b represents rainfall detected by the rain gauge but not by the RGD and c represents rainfall detected by the RGD but not by the rain gauge.

Statistical metrics	**Units**	**Equations**	**Perfect Values**
RMSE	mm/d	$\sqrt{\frac{\sum_{i=1}^{n}(Y_i - X_i)^2}{n}}$	0
R	–	$\frac{\sum_{i=1}^{n}(X_i - \overline{X})(Y_i - \overline{Y})}{\sqrt{\sum_{i=1}^{n}(X_i - \overline{X})^2}\sqrt{\sum_{i=1}^{n}(Y_i - \overline{Y})^2}}$	1
α	–	$\frac{\sqrt{\sum_{i=1}^{n}(Y_i - \overline{Y})^2}}{\sqrt{\sum_{i=1}^{n}(X_i - \overline{X})^2}}$	1
β	–	$\frac{\overline{Y}}{\overline{X}}$	1
KGE	–	$1 - \sqrt{(1-R)^2 + (1-\alpha)^2 + (1-\beta)^2}$	1
POD	–	$\frac{a}{a+b}$	1
FAR	–	$\frac{c}{a+c}$	0
CSI	–	$\frac{a}{a+b+c}$	1

Table A3
Summary table of statistics (mean values, maximum values and standard deviation) of some rainfall percentiles in the Greater and Lesser Antilles. The expression tr symbolizes the rainfall as a trace.

Data base	test	5%	25%	50%	75%	90%	95%	99%
Rain gauge	Mean	tr	tr	0.5	3.69	13	22	54
	max	tr	tr	4.33	12.9	29	42	92
	Standard deviation	tr	tr	0.9	2.66	6	8	13
MSWEP	Mean	0	tr	0.6	3.1	10	18	45
	max	0	tr	2.1	6.6	19	34	86
	Standard deviation	0	tr	0.5	1.7	4	7	17
ERA-5	Mean	tr	tr	1.5	3.4	8	11	23
	max	tr	tr	4.1	8.4	14	19	36
	Standard deviation	tr	tr	0.6	1.2	2	3	4
CHIRPS	Mean	0	0	0	1.8	14	26.3	65
	max	0	0	0	8.1	3	57	138
	Standard deviation	0	0	0	2.6	5	10	24
PERSIANN-CDR	Mean	0	0	0.2	3.4	10	18	40
	max	0	0	1.4	7.7	17	27	55
	Standard eviation	0	0	0.3	1.9	3	4	7

IMERG were evaluated using 103 rain gauges in the Lesser and Greater Antilles, with the aim of highlighting the qualities and shortcomings of these RGD on a daily timescale and to guide researchers in the choice of RGD to use for hydrometeorological applications in this study area. To our knowledge, this is the first work done on RGD data on daily timescale in this region. For hydrological applications in the Greater and Lesser Antilles or on a watershed scale, the use of MSWEP is recommended due to its high KGE score and high spatio-temporal resolution (0.1° and 3 h). On the other hand, CHIRPS, ERA-5, GPM IMERG and PERSIANN-CDR are not recommended due to their low KGE score and/or coarse spatial resolution, which are not appropriate for the Greater and Lesser Antilles countries. For climatological applications, mainly to calculate climatic indexes such as number of rainy days exceeding a threshold, number of consecutive rainy days, etc. ERA-5, GMP IMERG and MSWEP are recommended due to their better POD and CSI scores. MSWEP, CHIRPS and PERSIANN-CDR are recommended in the Greater and Lesser Antilles for research on water resources management for irrigation, energy production, industry, etc. due to their ability to represent the annual rainfall seasonality. For

applications on heavy rainfall statistics, CHIRPS and MSWEP are recommended for their good capacity to estimate the percentiles of heavy rainfall. In summary, MSWEP is recommended for most hydrometeorological applications in the study area because of its good performance for almost all statistical metrics and its good spatio-temporal resolution.

This work provides a guide to users of rainfall data in the Lesser and Greater Antilles on their choice of RGD to use in countries with very limited rainfall data, such as Haiti, taking into account the benefits and drawbacks of each RGD. The evaluation of these RGD performances might be extended on the studied region using other validation metrics based on different parameters such as satellite-derived soil moisture products or rainfall-runoff modeling (Gampe and Ludwig, 2017; Musie et al., 2019). No tests have evaluated the RGD performance in measuring light rainfall, which would be useful for drought monitoring. This work could be a good direction for future research. Finally, the use of such RGD as inputs of rainfall-runoff models for flood forecasting, flood mapping or hydraulic structure design is an interesting application of this work.

CRediT authorship contribution statement

Bathelemy Ralph: Conceptualization, Methodology, Software, Data curation, Writing – original draft preparation, Writing. **Brigode Pierre** Validation, Supervision, Project administration, Writing – review & editing. **Boisson Dominique:** Validation, Supervision, Writing – review & editing. **Tric Emmanuel:** Validation, Supervision, Writing – review & editing.

Declaration of Competing Interest

The authors declare that they have no known competing financial interests or personal relationships that could have appeared to influence the work reported in this paper.

Acknowledgements

The authors thank all weather services that provided rainfall data. In particular, Météo-France for rainfall data from Guadeloupe and Martinique, UHM for rainfall data from Haiti, InsMet for rainfall data from Cuba, ONAMET for rainfall data from Dominican Republic, CIMH for rainfall data from several Caribbean islands, MetService for rainfall data from Jamaica and NOAA for rainfall data from Puerto Rico. Special acknowledgement to Cedric Van Meerbeeck and Adrian Trotman who helped us to find the contacts of some weather services in the Caribbean and to Hylke E. Beck for the MSWEP data. The PhD thesis of Ralph BATHELEMY is funded by the French Embassy in Haiti and Institut de Recherche pour le Développement (the French National Research Institute for Sustainable Development). This work is a contribution to the International Joint Laboratory CARIBACT. The authors thank the three reviewers and the editor who provided constructive comments on an earlier version of the manuscript, which helped clarify the text.

Appendix

See. Fig. A1, Fig. A2 and Fig. A3.
See. Table A1, Table. 2 and Table A3.

References

Adler, R.F., Huffman, G.J., Chang, A., Ferraro, R., Xie, P.-P., Janowiak, J., Rudolf, B., Schneider, U., Curtis, S., Bolvin, D., Gruber, A., Susskind, J., Arkin, P., Nelkin, E., 2003. The version-2 global precipitation climatology project (GPCP) monthly precipitation analysis (1979–Present). J. Hydrometeorol. 4, 1147–1167. https://doi.org/10.1175/1525-7541(2003)004<1147:TVGPCP>2.0.CO;2.

Agudelo, P.A., Hoyos, C.D., Curry, J.A., Webster, P.J., 2011. Probabilistic discrimination between large-scale environments of intensifying and decaying African easterly waves. Clim. Dyn. 36, 1379–1401. https://doi.org/10.1007/s00382-010-0851-x.

Alijanian, M., Rakhshandehroo, G.R., Mishra, A.K., Dehghani, M., 2017. Evaluation of satellite rainfall climatology using CMORPH, PERSIANN-CDR, PERSIANN, TRMM, MSWEP over Iran. Int. J. Clim. 37, 4896–4914. https://doi.org/10.1002/joc.5131.

Angeles, M.E., González, J.E., Ramírez-Beltrán, N.D., Tepley, C.A., Comarazamy, D.E., 2010. Origins of the Caribbean rainfall bimodal behavior. J. Geophys. Res. Atmospheres 115. https://doi.org/10.1029/2009JD012990.

Arciniega-Esparza, S., Birkel, C., Chavarría-Palma, A., Arheimer, B., Breña-Naranjo, J.A., 2022. Remote sensing-aided rainfall–runoff modeling in the tropics of Costa Rica. Hydrol. Earth Syst. Sci. 26, 975–999. https://doi.org/10.5194/hess-26-975-2022.

Ashouri, H., Hsu, K.-L., Sorooshian, S., Braithwaite, D.K., Knapp, K.R., Cecil, L.D., Nelson, B.R., Prat, O.P., 2015. PERSIANN-CDR: daily precipitation climate data record from multisatellite observations for hydrological and climate studies. Bull. Am. Meteorol. Soc. 96, 69–83. https://doi.org/10.1175/BAMS-D-13-00068.1.

Baez-Villanueva, O.M., Zambrano-Bigiarini, M., Ribbe, L., Nauditt, A., Giraldo-Osorio, J.D., Thinh, N.X., 2018. Temporal and spatial evaluation of satellite rainfall estimates over different regions in Latin-America. Atmos. Res. 213, 34–50. https://doi.org/10.1016/j.atmosres.2018.05.011.

Beck, H.E., Dijk, A.I.J.M., van, Levizzani, V., Schellekens, J., Miralles, D.G., Martens, B., Roo, A. de, 2017. MSWEP: 3-hourly 0.25° global gridded precipitation (1979-2015) by merging gauge, satellite, and reanalysis data. Hydrol. Earth Syst. Sci. 21, 589–615. https://doi.org/10.5194/hess-21-589-2017.

Beck, H.E., Wood, E.F., Pan, M., Fisher, C.K., Miralles, D.G., Dijk, A.I.J.M., van, McVicar, T.R., Adler, R.F., 2019. MSWEP V2 Global 3-Hourly 0.1° precipitation: methodology and quantitative assessment. Bull. Am. Meteorol. Soc. 100, 473–500. https://doi.org/10.1175/BAMS-D-17-0138.1.

Bois, P., 1987. Contrôle de séries chronologiques corrélées par étude du cumul des résidus de la corrélation. ORSTOM.

Bozza, A., Durand, A., Confortola, G., Soncini, A., Allenbach, B., Bocchiola, D., 2016. Potential of remote sensing and open street data for flood mapping in poorly gauged areas: a case study in Gonaives, Haiti. Appl. Geomat. 8, 117–131. https://doi.org/10.1007/s12518-016-0171-x.

Brochart, D., Andréassian, V., 2014. Correction des estimations des pluies par satellite pour les bassins versants de Guyane française. Bull. Séances Académie R. Sci. O.-M. 60, 361–370.

Burgess, C.P., Taylor, M.A., Spencer, N., Jones, J., Stephenson, T.S., 2018. Estimating damages from climate-related natural disasters for the Caribbean at 1.5 °C and 2 °C global warming above preindustrial levels. Reg. Environ. Change 18, 2297–2312. https://doi.org/10.1007/s10113-018-1423-6.

Cantet, P., 2017. Mapping the mean monthly precipitation of a small island using kriging with external drifts. Theor. Appl. Climatol. 127, 31–44. https://doi.org/10.1007/s00704-015-1610-z.

Centella-Artola, A., Bezanilla-Morlot, A., Taylor, M.A., Herrera, D.A., Martinez-Castro, D., Gouirand, I., Sierra-Lorenzo, M., Vichot-Llano, A., Stephenson, T., Fonseca, C., Campbell, J., Alpizar, M., 2020. Evaluation of Sixteen Gridded Precipitation Datasets over the Caribbean Region Using Gauge Observations. Atmosphere 11, 1334. https://doi.org/10.3390/atmos11121334.

Cook, K.H., Vizy, E.K., 2010. Hydrodynamics of the Caribbean low-level jet and its relationship to precipitation. J. Clim. 23, 1477–1494. https://doi.org/10.1175/2009JCLI3210.1.

Daly, C., Helmer, E.H., Quiñones, M., 2003. Mapping the climate of Puerto Rico. Vieques Culebra. Int. J. Clim. 23, 1359–1381. https://doi.org/10.1002/joc.937.

Davis, R.E., Hayden, B.P., Gay, D.A., Phillips, W.L., Jones, G.V., 1997. The North Atlantic subtropical anticyclone. J. Clim. 10, 728–744. https://doi.org/10.1175/1520-0442(1997)010<0728:TNASA>2.0.CO;2.

Dee, D.P., Uppala, S.M., Simmons, A.J., Berrisford, P., Poli, P., Kobayashi, S., Andrae, U., Balmaseda, M.A., Balsamo, G., Bauer, P., Bechtold, P., Beljaars, A.C.M., Berg, L., van de, Bidlot, J., Bormann, N., Delsol, C., Dragani, R., Fuentes, M., Geer, A.J., Haimberger, L., Healy, S.B., Hersbach, H., Hólm, E.V., Isaksen, L., Kållberg, P., Köhler, M., Matricardi, M., McNally, A.P., Monge-Sanz, B.M., Morcrette, J.-J., Park, B.-K., Peubey, C., Rosnay, P., de, Tavolato, C., Thépaut, J.-N., Vitart, F., 2011. The ERA-Interim reanalysis: configuration and performance of the data assimilation system. Q. J. R. Meteorol. Soc. 137, 553–597. https://doi.org/10.1002/qj.828.

Dinku, T., Ceccato, P., Grover-Kopec, E., Lemma, M., Connor, S.J., Ropelewski, C.F., 2007. Validation of satellite rainfall products over East Africa's complex topography. Int. J. Remote Sens 28, 1503–1526. https://doi.org/10.1080/01431160600954688.

Fang, J., Yang, W., Luan, Y., Du, J., Lin, A., Zhao, L., 2019. Evaluation of the TRMM 3B42 and GPM IMERG products for extreme precipitation analysis over China. Atmos. Res. 223, 24–38. https://doi.org/10.1016/j.atmosres.2019.03.001.

Fick, S.E., Hijmans, R.J., 2017. WorldClim 2: new 1-km spatial resolution climate surfaces for global land areas. Int. J. Climatol. 37, 4302–4315. https://doi.org/10.1002/joc.5086.

Funk, C., Peterson, P., Landsfeld, M., Pedreros, D., Verdin, J., Shukla, S., Husak, G., Rowland, J., Harrison, L., Hoell, A., Michaelsen, J., 2015. The climate hazards infrared precipitation with stations—a new environmental record for monitoring extremes. Sci. Data 2, 150066. https://doi.org/10.1038/sdata.2015.66.

Gampe, D., Ludwig, R., 2017. Evaluation of gridded precipitation data products for hydrological applications in complex topography. Hydrology 4, 53. https://doi.org/10.3390/hydrology4040053.

Griffith, C.G., Woodley, W.L., Grube, P.G., Martin, D.W., Stout, J., Sikdar, D.N., 1978. Rain estimation from geosynchronous satellite imagery—visible and infrared studies. Mon. Weather Rev. 106, 1153–1171. https://doi.org/10.1175/1520-0493(1978)106<1153:REFGSI>2.0.CO;2.

Gupta, H.V., Kling, H., Yilmaz, K.K., Martinez, G.F., 2009. Decomposition of the mean squared error and NSE performance criteria: Implications for improving hydrological modelling. J. Hydrol. 377, 80–91. https://doi.org/10.1016/j.jhydrol.2009.08.003.

Habib, E., Larson, B.F., Graschel, J., 2009. Validation of NEXRAD multisensor precipitation estimates using an experimental dense rain gauge network in south Louisiana. J. Hydrol. 373, 463–478. https://doi.org/10.1016/j.jhydrol.2009.05.010.

Hastenrath, S., 2002. The intertropical convergence zone of the eastern Pacific revisited. Int. J. Climatol. 22, 347–356. https://doi.org/10.1002/joc.739.

Hersbach, H., De Rosnay, B.B.S., 2018. Operational global reanalysis: progress, future directions and synergies with NWP (ERA Report Series No. 27). ERA Report. ECMWF.

Hersbach, H., Bell, B., Berrisford, P., Hirahara, S., Horányi, A., Muñoz-Sabater, J., Nicolas, J., Peubey, C., Radu, R., Schepers, D., Simmons, A., Soci, C., Abdalla, S., Abellan, X., Balsamo, G., Bechtold, P., Biavati, G., Bidlot, J., Bonavita, M., Chiara, G.D., Dahlgren, P., Dee, D., Diamantakis, M., Dragani, R., Flemming, J., Forbes, R., Fuentes, M., Geer, A., Haimberger, L., Healy, S., Hogan, R.J., Hólm, E., Janisková, M., Keeley, S., Laloyaux, P., Lopez, P., Lupu, C., Radnoti, G., Rosnay, P., de, Rozum, I., Vamborg, F., Villaume, S., Thépaut, J.-N., 2020. The ERA5 global reanalysis. Q. J. R. Meteorol. Soc. 146, 1999–2049. https://doi.org/10.1002/qj.3803.

Hou, A.Y., Kakar, R.K., Neeck, S., Azarbarzin, A.A., Kummerow, C.D., Kojima, M., Oki, R., Nakamura, K., Iguchi, T., 2014. The global precipitation measurement mission. Bull. Am. Meteorol. Soc. 95, 701–722. https://doi.org/10.1175/BAMS-D-13-00164.1.

Huffman, G.J., Bolvin, D.T., Nelkin, E.J., Wolff, D.B., Adler, R.F., Gu, G., Hong, Y., Bowman, K.P., Stocker, E.F., 2007. The TRMM multisatellite precipitation analysis (TMPA): quasi-global, multiyear, combined-sensor precipitation estimates at fine scales. J. Hydrometeorol. 8, 38–55. https://doi.org/10.1175/JHM560.1.

Huffman, G.J., Bolvin, D.T., Braithwaite, D., Hsu, K., Joyce, R., Xie, P., Yoo, S.-H., 2015. NASA global precipitation measurement (GPM) integrated multi-satellite retrievals for GPM (IMERG). Algorithm Theor. Basis Doc. ATBD Version 4, 26.

Jarvis, A., Reuter, H.I., Nelson, A., Guevara, E., 2008. Hole-filled seamless SRTM data V4, International Centre for. Trop. Agric.

Jones, P.D., Harpham, C., Harris, I., Goodess, C.M., Burton, A., Centella-Artola, A., Taylor, M.A., Bezanilla-Morlot, A., Campbell, J.D., Stephenson, T.S., Joslyn, O., Nicholls, K., Baur, T., 2016. Long-term trends in precipitation and temperature across the Caribbean. Int. J. Climatol. 36, 3314–3333. https://doi.org/10.1002/joc.4557.

Joyce, R.J., Janowiak, J.E., Arkin, P.A., Xie, P., 2004. CMORPH: a method that produces global precipitation estimates from passive microwave and infrared data at high spatial and temporal resolution. J. Hydrometeorol. 5, 487–503. https://doi.org/10.1175/1525-7541(2004)005<0487:CAMTPG>2.0.CO;2.

Jury, M.R., 2009. An intercomparison of observational, reanalysis, satellite, and coupled model data on mean rainfall in the Caribbean. J. Hydrometeorol. 10, 413–430. https://doi.org/10.1175/2008JHM1054.1.

Jury, M.R., 2016. Inter-annual rainfall variability in the eastern Antilles and coupling with the regional and intra-seasonal circulation. Theor. Appl. Climatol. 126, 727–737. https://doi.org/10.1007/s00704-015-1612-x.

Khouakhi, A., Villarini, G., Vecchi, G.A., 2017. Contribution of tropical cyclones to rainfall at the global scale. J. Clim. 30, 359–372. https://doi.org/10.1175/JCLI-D-16-0298.1.

Kidd, C., Becker, A., Huffman, G.J., Muller, C.L., Joe, P., Skofronick-Jackson, G., Kirschbaum, D.B., 2017. So, how much of the Earth's surface is covered by rain gauges? Bull. Am. Meteorol. Soc. 98, 69–78. https://doi.org/10.1175/BAMS-D-14-00283.1.

Knapp, K.R., 2008. Scientific data stewardship of international satellite cloud climatology project B1 global geostationary observations. J. Appl. Remote Sens. 2, 023548 https://doi.org/10.1117/1.3043461.

Knapp, K.R., Ansari, S., Bain, C.L., Bourassa, M.A., Dickinson, M.J., Funk, C., Helms, C.N., Hennon, C.C., Holmes, C.D., Huffman, G.J., Kossin, J.P., Lee, H.-T., Loew, A., Magnusdottir, G., 2011. Globally gridded satellite observations for climate studies. Bull. Am. Meteorol. Soc. 92, 893–907. https://doi.org/10.1175/2011BAMS3039.1.

Kobayashi, S., Ota, Y., Harada, Y., Ebita, A., Moriya, M., Onoda, H., Onogi, K., Kamahori, H., Kobayashi, C., Endo, H., Miyaoka, K., Takahashi, K., 2015. The JRA-55 reanalysis: general specifications and basic characteristics. J. Meteorol. Soc. Jpn. Ser. II 93, 5–48. https://doi.org/10.2151/jmsj.2015-001.

Kuentz, A., Mathevet, T., Gailhard, J., Hingray, B., 2015. Building long-term and high spatio-temporal resolution precipitation and air temperature reanalyses by mixing local observations and global atmospheric reanalyses: the ANATEM model. Hydrol. Earth Syst. Sci. 19, 2717–2736. https://doi.org/10.5194/hess-19-2717-2015.

Li, X., Chen, Y., Deng, X., Zhang, Y., Chen, L., 2021. Evaluation and hydrological utility of the GPM IMERG precipitation products over the xinfengjiang river reservoir basin, China. Remote Sens 13, 866. https://doi.org/10.3390/rs13050866.

Li, Z., Yang, D., Gao, B., Jiao, Y., Hong, Y., Xu, T., 2015. Multiscale hydrologic applications of the latest satellite precipitation products in the yangtze river basin using a distributed hydrologic model. J. Hydrometeorol. 16, 407–426. https://doi.org/10.1175/JHM-D-14-0105.1.

Liu, J., Duan, Z., Jiang, J., Zhu, A.-X., 2015. Evaluation of three satellite precipitation products TRMM 3B42, CMORPH, and PERSIANN over a subtropical watershed in China. Adv. Meteorol. 2015, e151239 https://doi.org/10.1155/2015/151239.

Martinez, C., Goddard, L., Kushnir, Y., Ting, M., 2019. Seasonal climatology and dynamical mechanisms of rainfall in the Caribbean. Clim. Dyn. 53, 825–846. https://doi.org/10.1007/s00382-019-04616-4.

Mashingia, F., Mtalo, F., Bruen, M., 2014. Validation of remotely sensed rainfall over major climatic regions in Northeast Tanzania. Phys. Chem. Earth Parts ABC 67–69, 55–63. https://doi.org/10.1016/j.pce.2013.09.013.

Mathevet, T., Gupta, H., Perrin, C., Andréassian, V., Le Moine, N., 2020. Assessing the performance and robustness of two conceptual rainfall-runoff models on a worldwide sample of watersheds. J. Hydrol. 585, 124698 https://doi.org/10.1016/j.jhydrol.2020.124698.

Mazzoleni, M., Brandimarte, L., Amaranto, A., 2019. Evaluating precipitation datasets for large-scale distributed hydrological modelling. J. Hydrol. 578, 124076 https://doi.org/10.1016/j.jhydrol.2019.124076.

Menne, M.J., Durre, I., Vose, R.S., Gleason, B.E., Houston, T.G., 2012. An overview of the global historical climatology network-daily database. J. Atmos. Ocean. Technol. 29, 897–910. https://doi.org/10.1175/JTECH-D-11-00103.1.

Moron, V., Frelat, R., Jean-Jeune, P.K., Gaucherel, C., 2015. Interannual and intra-annual variability of rainfall in Haiti (1905–2005. Clim. Dyn. 45, 915–932. https://doi.org/10.1007/s00382-014-2326-y.

Moron, V., Gouirand, I., Taylor, M., 2016. Weather types across the Caribbean basin and their relationship with rainfall and sea surface temperature. Clim. Dyn. 47, 601–621. https://doi.org/10.1007/s00382-015-2858-9.

Musie, M., Sen, S., Srivastava, P., 2019. Comparison and evaluation of gridded precipitation datasets for streamflow simulation in data scarce watersheds of Ethiopia. J. Hydrol. 579, 124168 https://doi.org/10.1016/j.jhydrol.2019.124168.

Peterson, T.C., Taylor, M.A., Demeritte, R., Duncombe, D.L., Burton, S., Thompson, F., Porter, A., Mercedes, M., Villegas, E., Fils, R.S., Tank, A.K., Martis, A., Warner, R., Joyette, A., Mills, W., Alexander, L., Gleason, B., 2002. Recent changes in climate extremes in the Caribbean region. ACL 16-1-ACL 16-9 J. Geophys. Res. Atmospheres 107. https://doi.org/10.1029/2002JD002251.

Pradhan, A., Nair, A.S., Indu, J., Kirstetter, P.-E., 2021. Impact of sampling of GPM orbital data on streamflow simulations. J. Hydrol. 593, 125798 https://doi.org/10.1016/j.jhydrol.2020.125798.

Pradhan, R.K., Markonis, Y., Vargas Godoy, M.R., Villalba-Pradas, A., Andreadis, K.M., Nikolopoulos, E.I., Papalexiou, S.M., Rahim, A., Tapiador, F.J., Hanel, M., 2022. Review of GPM IMERG performance: a global perspective. Remote Sens. Environ. 268, 112754 https://doi.org/10.1016/j.rse.2021.112754.

Prakash, S., 2019. Performance assessment of CHIRPS, MSWEP, SM2RAIN-CCI, and TMPA precipitation products across India. J. Hydrol. 571, 50–59. https://doi.org/10.1016/j.jhydrol.2019.01.036.

Saemian, P., Hosseini-Moghari, S.-M., Fatehi, I., Shoarinezhad, V., Modiri, E., Tourian, M.J., Tang, Q., Nowak, W., Bárdossy, A., Sneeuw, N., 2021. Comprehensive evaluation of precipitation datasets over Iran. J. Hydrol. 603, 127054 https://doi.org/10.1016/j.jhydrol.2021.127054.

Schneider, U., Becker, A., Finger, P., Meyer-Christoffer, A., Ziese, M., Rudolf, B., 2014. GPCC's new land surface precipitation climatology based on quality-controlled in situ data and its role in quantifying the global water cycle. Theor. Appl. Climatol. 115, 15–40. https://doi.org/10.1007/s00704-013-0860-x.

Sevruk, B., Ondrás, M., Chvíla, B., 2009. The WMO precipitation measurement intercomparisons. Atmospheric Res., 7th International Workshop on Precipitation in Urban Areas 92, 376–380. https://doi.org/10.1016/j.atmosres.2009.01.016.

Sharif, R.B., Habib, E.H., ElSaadani, M., 2020. Evaluation of radar-rainfall products over coastal Louisiana. Remote Sens 12, 1477. https://doi.org/10.3390/rs12091477.

Sharifi, E., Eitzinger, J., Dorigo, W., 2019. Performance of the state-of-the-art gridded precipitation products over mountainous terrain: a regional study over Austria. Remote Sens 11, 2018. https://doi.org/10.3390/rs11172018.

Smith, R.B., Minder, J.R., Nugent, A.D., Storelvmo, T., Kirshbaum, D.J., Warren, R., Lareau, N., Palany, P., James, A., French, J., 2012. Orographic precipitation in the tropics: the dominica experiment. Bull. Am. Meteorol. Soc. 93, 1567–1579. https://doi.org/10.1175/BAMS-D-11-00194.1.

Stampoulis, D., Anagnostou, E.N., 2012. Evaluation of global satellite rainfall products over continental Europe. J. Hydrometeorol. 13, 588–603. https://doi.org/10.1175/JHM-D-11-086.1.

Sultana, R., Nasrollahi, N., 2018. Evaluation of remote sensing precipitation estimates over Saudi Arabia. J. Arid Environ. 151, 90–103. https://doi.org/10.1016/j.jaridenv.2017.11.002.

Tan, M.L., Santo, H., 2018. Comparison of GPM IMERG, TMPA 3B42 and PERSIANN-CDR satellite precipitation products over Malaysia. Atmos. Res. 202, 63–76. https://doi.org/10.1016/j.atmosres.2017.11.006.

Tan, M.L., Ibrahim, A.L., Duan, Z., Cracknell, A.P., Chaplot, V., 2015. Evaluation of six high-resolution satellite and ground-based precipitation products over Malaysia. Remote Sens 7, 1504–1528. https://doi.org/10.3390/rs70201504.

Tang, G., Clark, M.P., Papalexiou, S.M., Ma, Z., Hong, Y., 2020. Have satellite precipitation products improved over last two decades? a comprehensive comparison of GPM IMERG with nine satellite and reanalysis datasets. Remote Sens. Environ. 240, 111697 https://doi.org/10.1016/j.rse.2020.111697.

Tang, X., Zhang, J., Gao, C., Ruben, G.B., Wang, G., 2019. Assessing the uncertainties of four precipitation products for swat modeling in Mekong River Basin. Remote Sens 11, 304. https://doi.org/10.3390/rs11030304.

Thorncroft, C., Hodges, K., 2001. African easterly wave variability and its relationship to atlantic tropical cyclone activity. J. Clim. 14, 1166–1179. https://doi.org/10.1175/1520-0442(2001)014<1166:AEWVAI>2.0.CO;2.

Ushio, T., Sasashige, K., Kubota, T., Shige, S., Okamoto, K., Aonashi, K., Inoue, T., Takahashi, N., Iguchi, T., Kachi, M., Oki, R., Morimoto, T., Kawasaki, Z.-I., 2009. A kalman filter approach to the global Satellite mapping of precipitation (GSMaP) from combined passive microwave and infrared radiometric data. J. Meteorol. Soc. Jpn. Ser. II 87A, 137–151. https://doi.org/10.2151/jmsj.87A.137.

Vila, D.A., de Goncalves, L.G.G., Toll, D.L., Rozante, J.R., 2009. Statistical evaluation of combined daily gauge observations and rainfall satellite estimates over continental South America. J. Hydrometeorol. 10, 533–543. https://doi.org/10.1175/2008JHM1048.1.

Villarini, G., Mandapaka, P.V., Krajewski, W.F., Moore, R.J., 2008. Rainfall and sampling uncertainties: a rain gauge perspective. J. Geophys. Res. Atmospheres 113. https://doi.org/10.1029/2007JD009214.

Viney, N.R., Bates, B.C., 2004. It never rains on Sunday: the prevalence and implications of untagged multi-day rainfall accumulations in the Australian high quality data set. Int. J. Clim. 24, 1171–1192. https://doi.org/10.1002/joc.1053.

Wang, C., Enfield, D.B., 2003. A further study of the tropical western hemisphere warm pool. J. Clim. 16, 1476–1493. https://doi.org/10.1175/1520-0442-16.10.1476.

Wang, C., Si, J., Zhao, C., Jia, B., Celestin, S., Li, D., He, X., Zhou, D., Qin, J., Zhu, X., 2022. Adequacy of satellite derived data for streamflow simulation in three Hexi inland river basins, Northwest China. Atmos. Res. 274, 106203 https://doi.org/10.1016/j.atmosres.2022.106203.

Wannasin, C., Brauer, C.C., Uijlenhoet, R., van Verseveld, W.J., Weerts, A.H., 2021. Daily flow simulation in Thailand Part I: Testing a distributed hydrological model with seamless parameter maps based on global data. J. Hydrol. Reg. Stud. 34, 100794 https://doi.org/10.1016/j.ejrh.2021.100794.

Xu, R., Tian, F., Yang, L., Hu, H., Lu, H., Hou, A., 2017. Ground validation of GPM IMERG and TRMM 3B42V7 rainfall products over southern Tibetan. Plateau Based a High. -Density Rain Gauge Netw. J. Geophys. Res. Atmospheres 122, 910–924. https://doi.org/10.1002/2016JD025418.